Interaction of high flux plasma with RAFM steels: experimental and computational assessment

(Eurofer 97 and advanced grades improved by thermomechanical treatment)

Dmitry Terentyev, Lorenzo Malerba, Athina Puype, Anastasia Bakaeva

SCK-CEN, Belgian Nuclear Research Centre

UNIVERSITEIT GENT

STUDIECENTRUM VOOR KERNENERGIE
CENTRE D'ETUDE DE L'ENERGIE NUCLEAIRE

SCK•CEN in short

- Cradle of Belgian nuclear research, applications and energy development in Belgium
- Major international player in the field of nuclear R&D
- ~700 staff, >50% with academic degree + 70 PhD students
- Annual turnover: 140 M€
  - 45% government support
  - 55% contract work

Outline

- Part I
  - Non-equilibrium D trapping under high flux plasma exposure: lessons learned by studying Tungsten
  - Computational model to consider Non-equilibrium trapping and its connection to diffusion limited trapping
  - Essential information from atomistic scale
- Part II
  - Standard and improved high-Cr grades
  - Available improved 9-Cr batches
  - Preliminary tests including high flux plasma exposure
- Work plan

Part I

- Part I
  - Non-equilibrium D trapping under high flux plasma exposure: lessons learned by studying Tungsten
  - Computational model to consider Non-equilibrium trapping and its connection to diffusion limited trapping
  - Essential information from atomistic scale

Experimental data

- Typical penetration depth ~ several μm
- Intensive blistering with pronounced by-modal size distribution
- TDS spectra: 3 release stages
- Intensity of the high T stage correlates with blister pattern

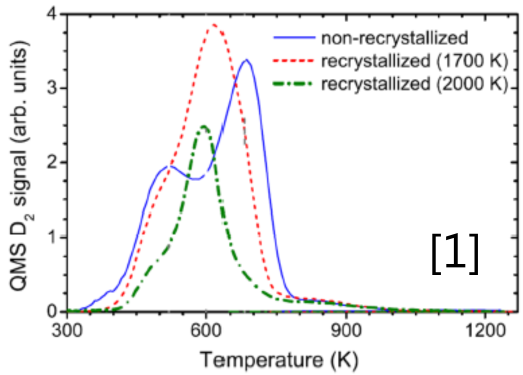

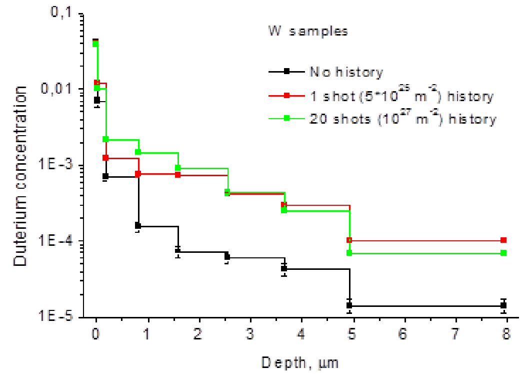

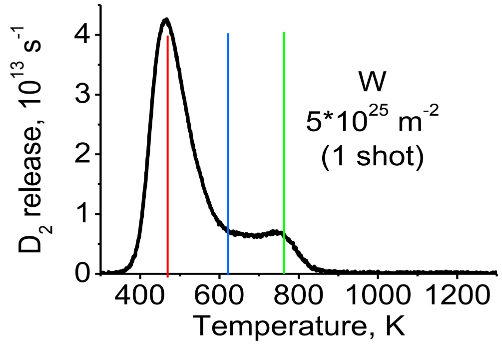

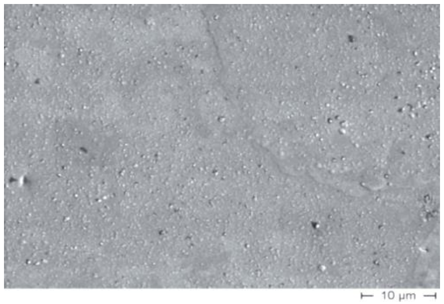

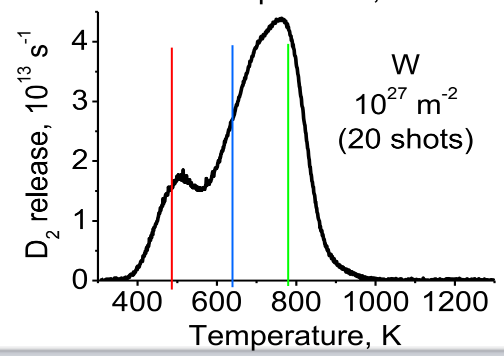

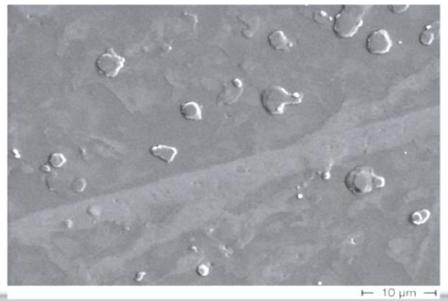

[1] M. Balden, S. Lindig, A. Manhard, J.-H. You, Journal of Nuclear Materials 414 (2011) 69-72.

Depth distribution & sub-surface trapping

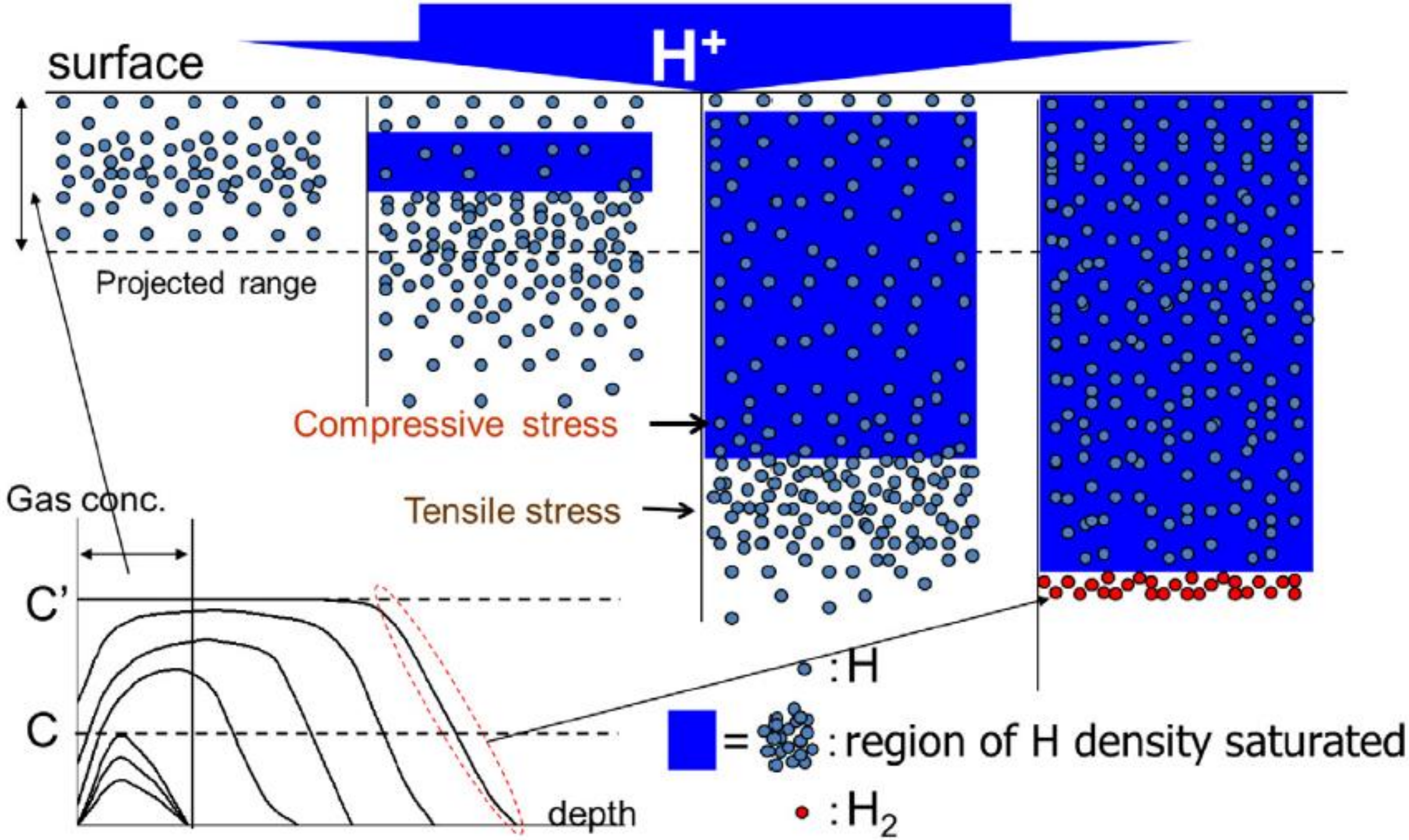

Tanabe et.al.

Depth distribution

- Three zones defining distribution
  - ~nm
  - ~ µm
  - ~ mm

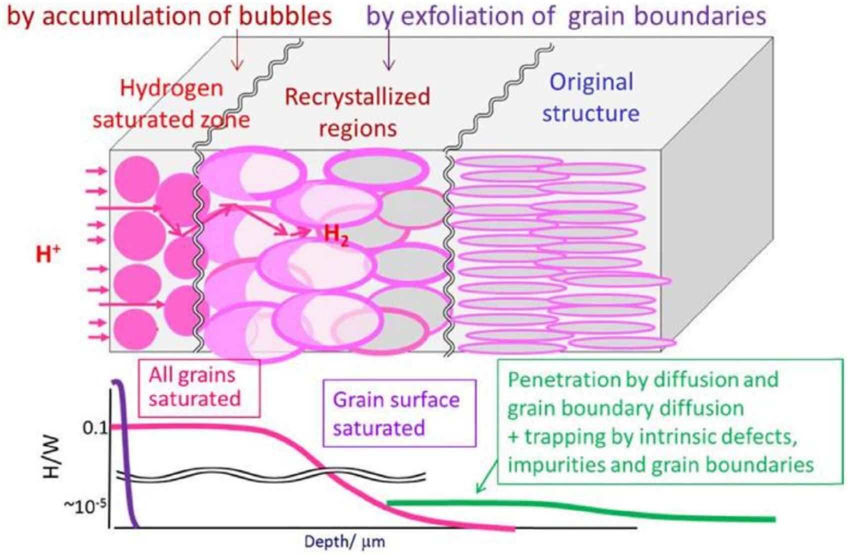

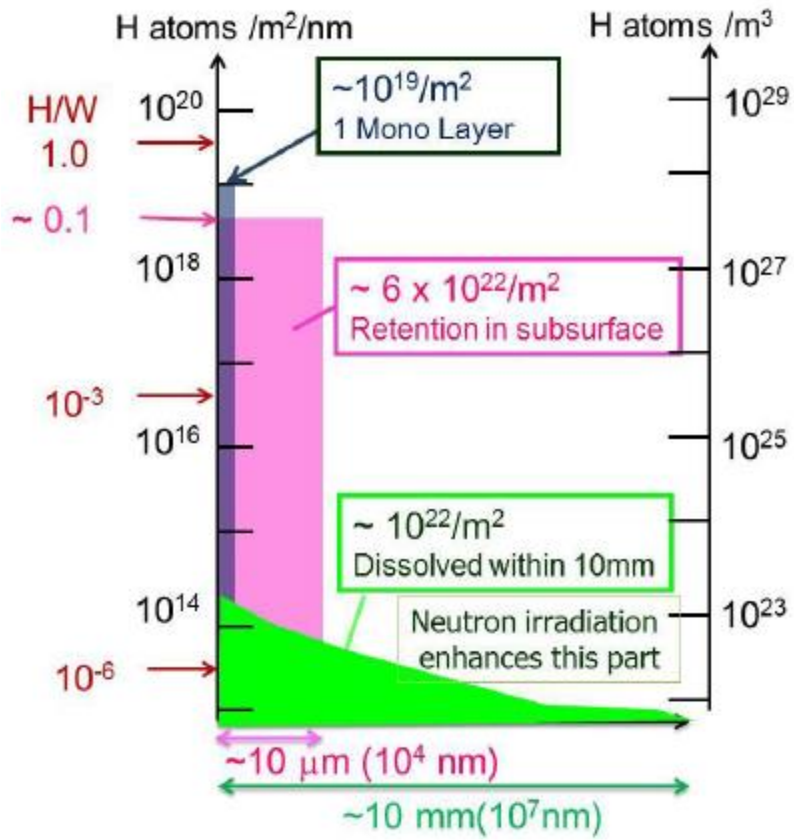

Tanabe et.al.

High heat flux plasma exposures

- PILOT-PSI (NL, DIFFER)
- Stationary Loads & ELM-like pulses
- B field = 0.4-1.6 T
- Water cooling 20 C

(passive control of T surface)

- Flux 10^{23}-10^{24} D/m^2

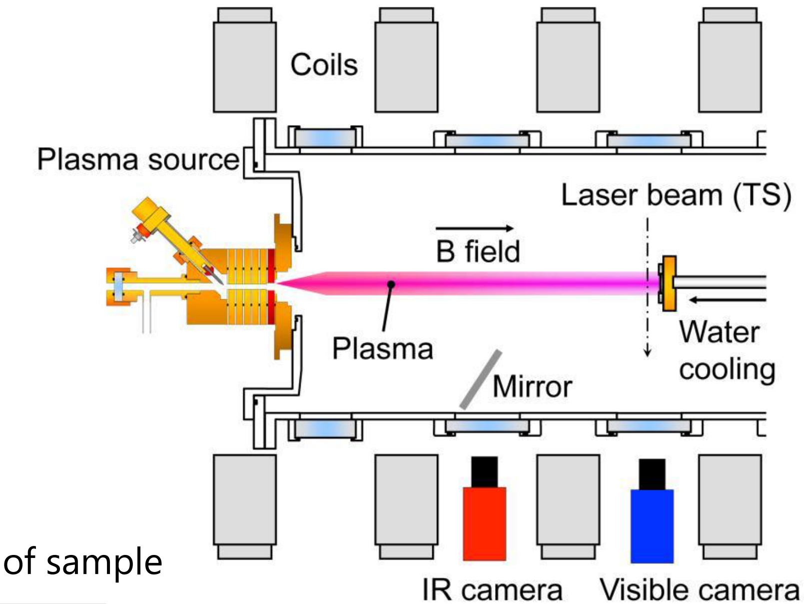

Temperature at the centre of sample

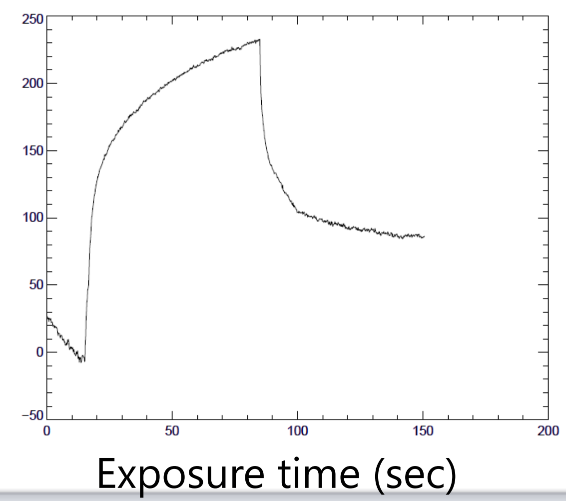

Typical ion flux profile

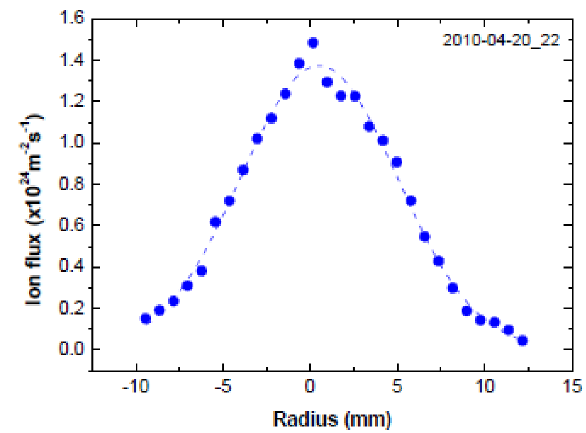

High flux plasma changes sub-surface

- Compressive stresses in sub-surface region generate:
  - Dense dislocation network
  - Limited within 10-15 µm
- Poly-crystalline (ITER-specification)

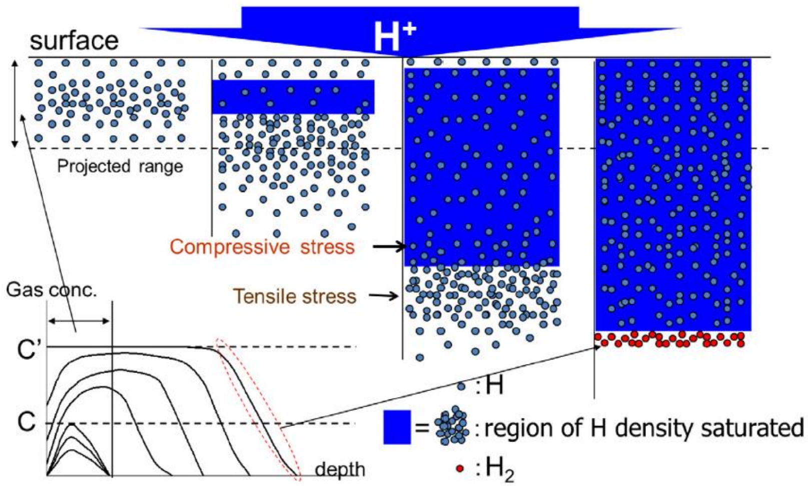

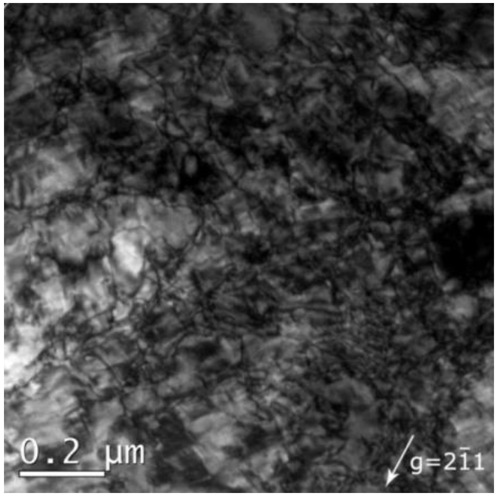

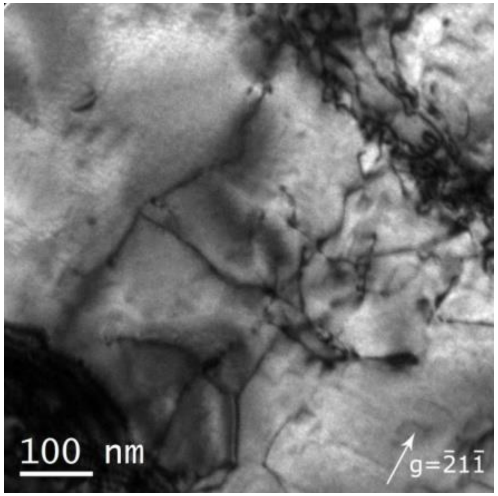

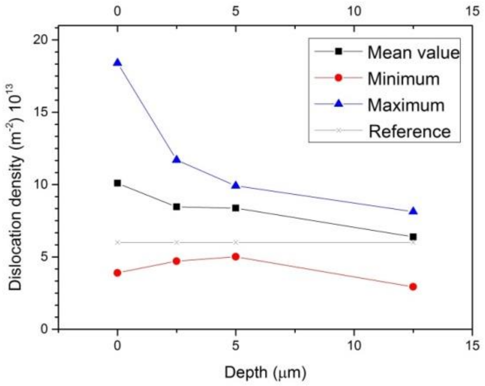

High flux plasma changes sub-surface

- Compressive stresses in sub-surface region generate:
  - Dense dislocation network
  - Limited within 10-15 µm
- Poly-crystalline (ITER-specification)
  - Recrystallized at 1600C (1h)

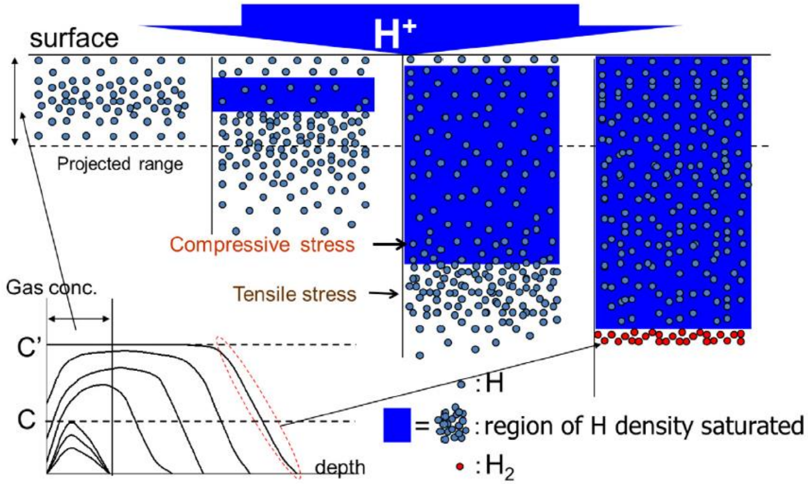

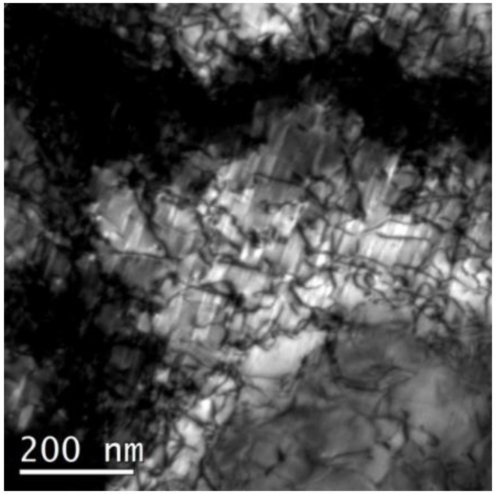

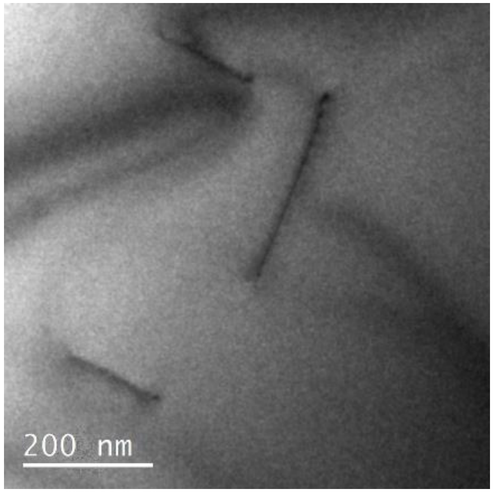

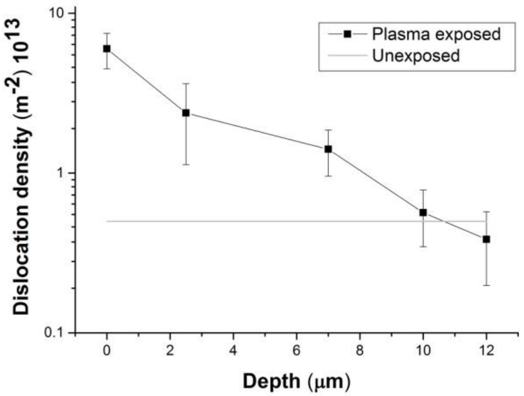

High flux plasma changes sub-surface

- Compressive stresses in sub-surface region generate:
  - Dense dislocation network
  - Limited within 10-15 μm

- Single crystal (110 orientation)

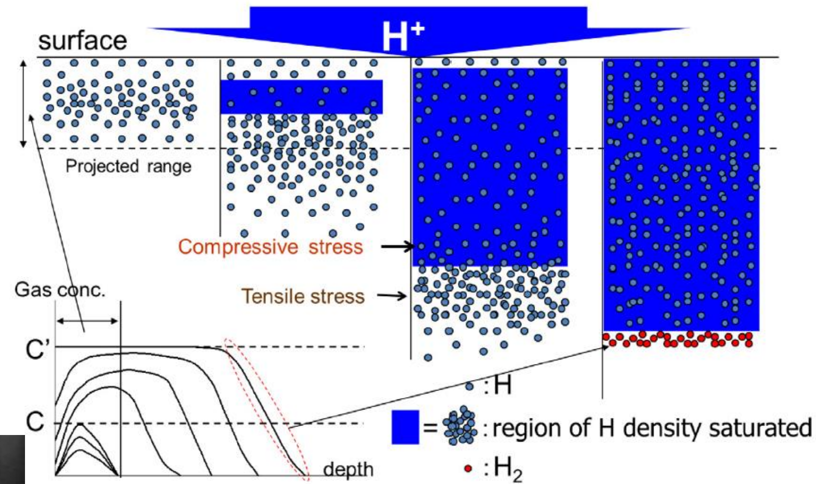

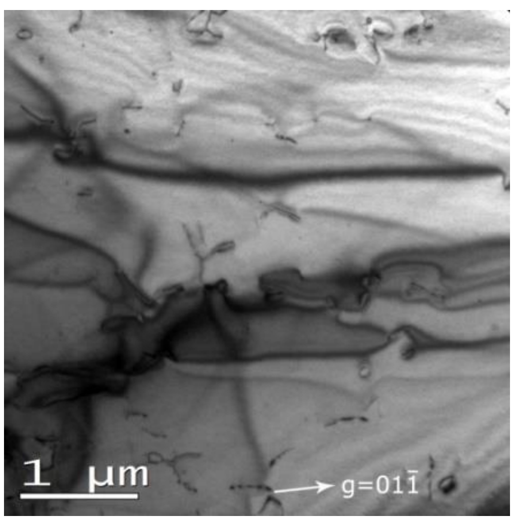

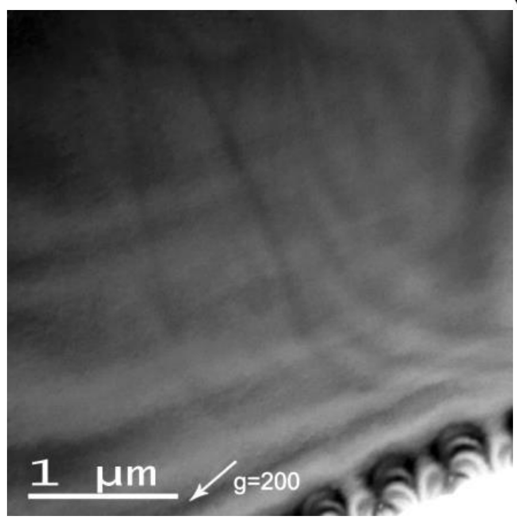

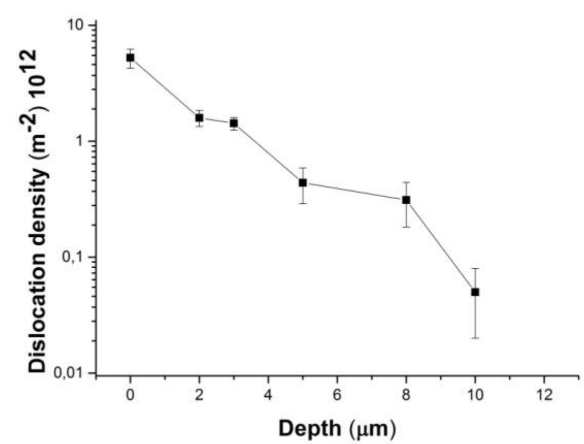

Experimental data

TEM sample

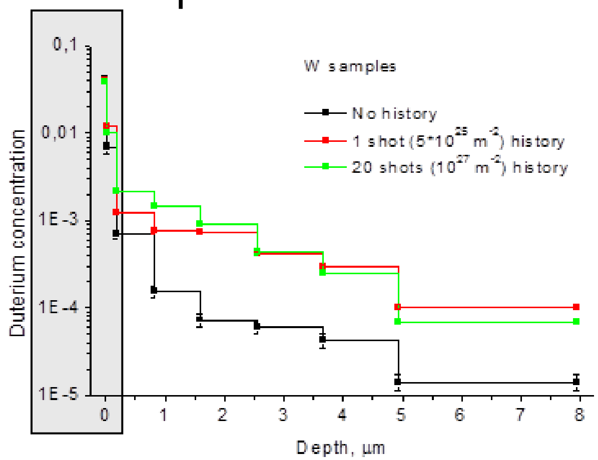

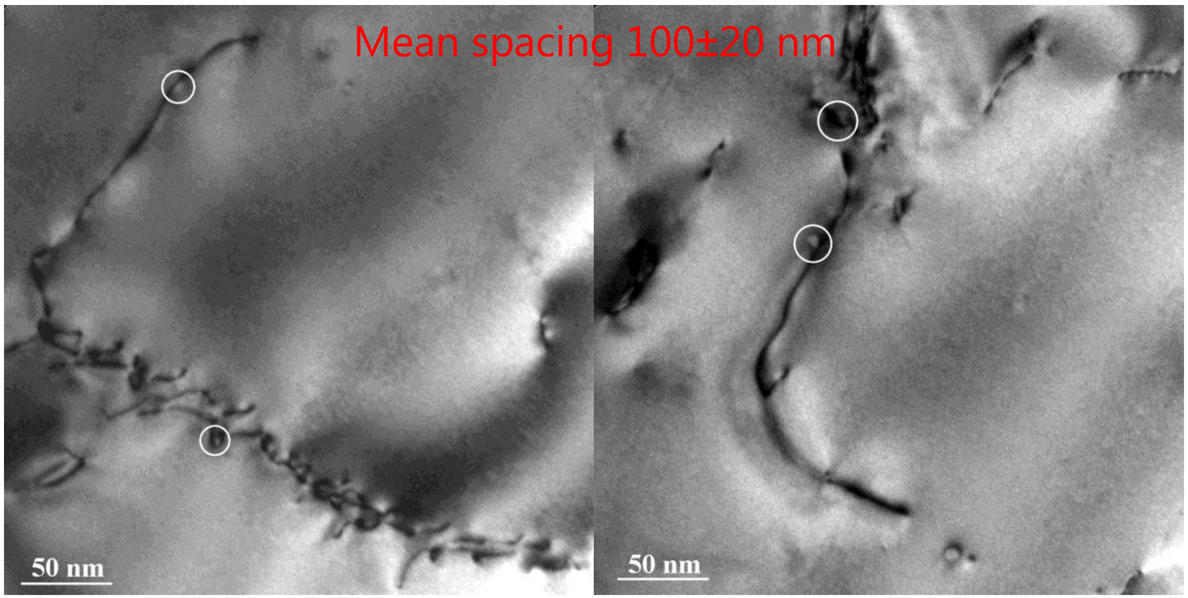

NRA range

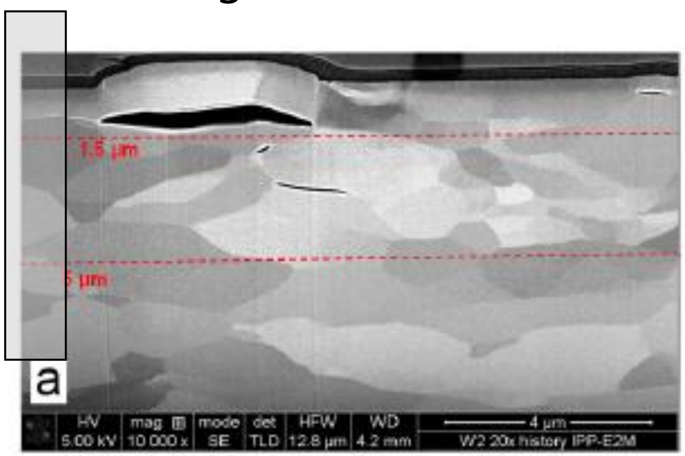

SEM edge on image

TEM image: 100-200 nm of top surface

Random grain boundaries

Low angle grain boundaries (LAGB

Dislocations

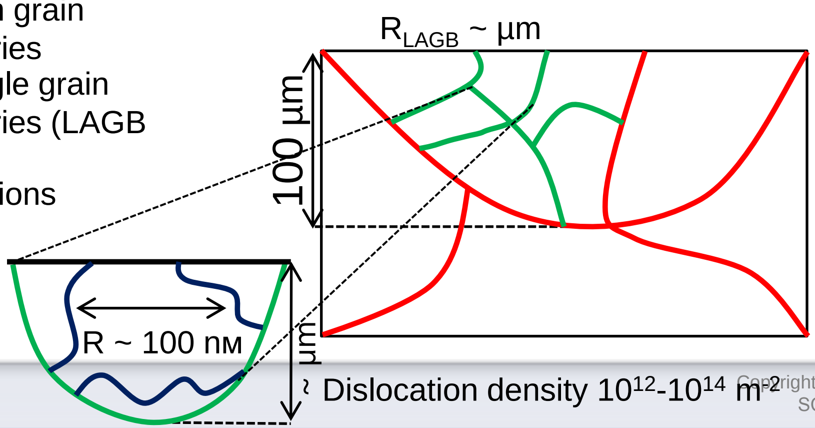

~ Dislocation density 10^{12}-10^{14} m^{-2}

Experimental data

- Select large grain (pre-characterized) material:
  Recrystallized W
- Perform controlled deformation:
  Tensile test on macro sample
- Sub-threshold plasma exposure:
  PILOT PSI, T=470K, flux ~10^{25} $D^2/m^2/sec$
- Exposure flux: 10, 70, 500 sec i.e. up to 5×10^{27}
- PIE sequence: SEM; TEM; TDS; SEM

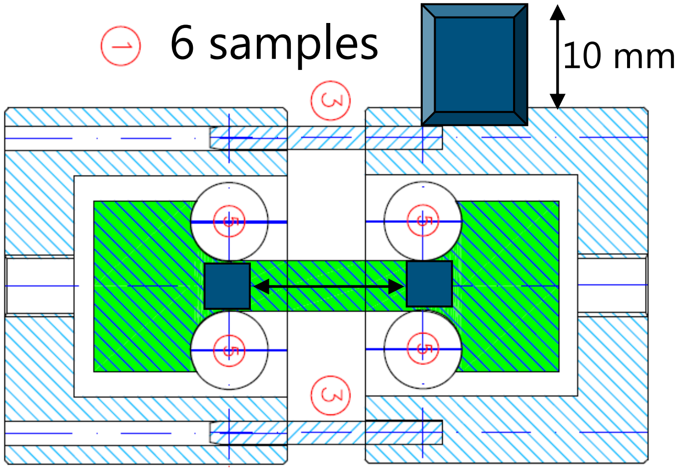

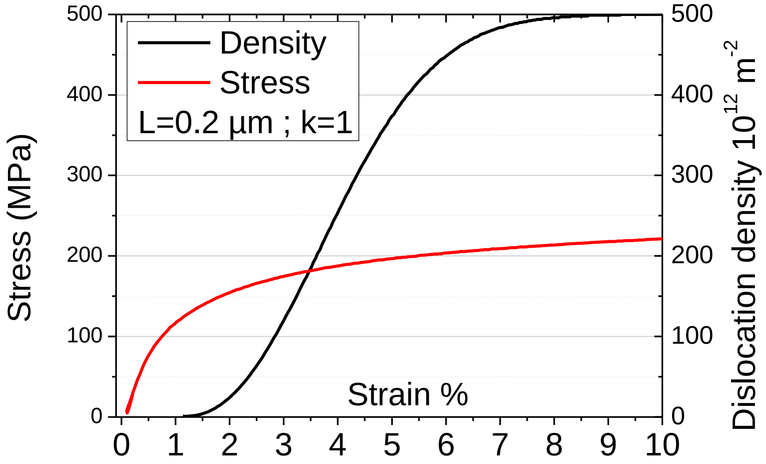

Strain hardening model by Meckin and Cocks [1]

$$\sigma_{d-d}(\varepsilon_p) = M\alpha\mu b\sqrt{\rho(\varepsilon_p)}$$

$$d\rho/d\varepsilon_p = M(1/bL - k\rho)$$

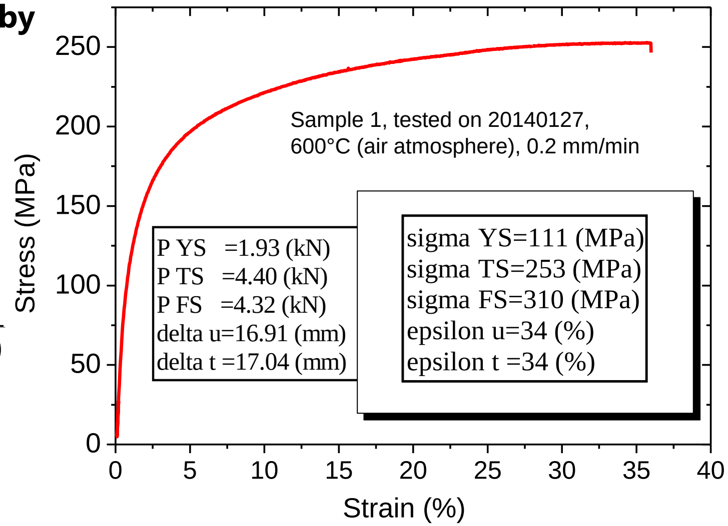

[1] H. Mecking, U.F. Kocks, Acta Metal. 29 (1981) 1865; [2] H. Sheng, G. Van Oost, et.al., J. Nucl. Mat. 444 (2014) 214.

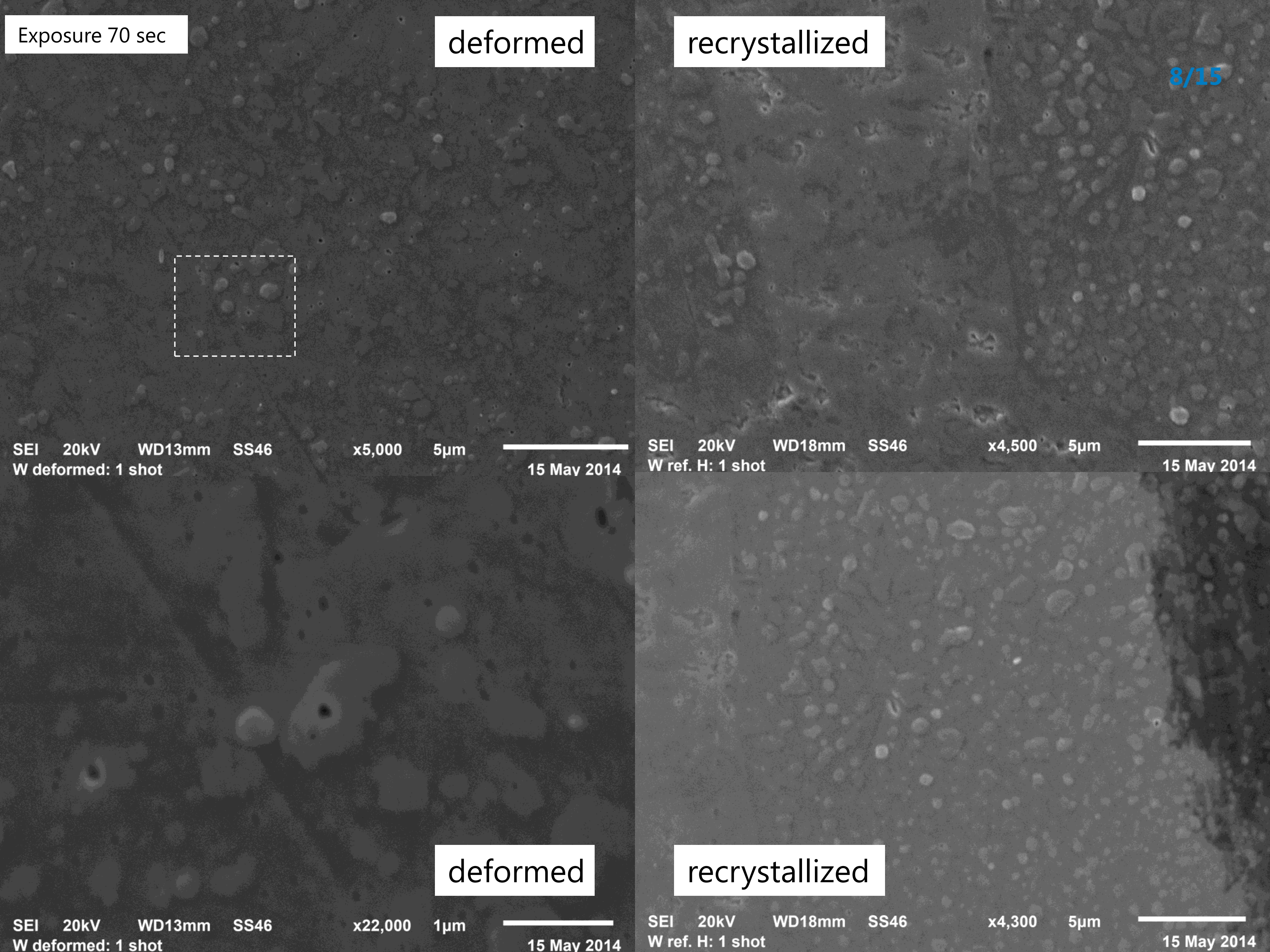
Exposure 70 sec
deformed
SEI 20kV WD13mm SS46 x5,000 5μm
W deformed: 1 shot 15 May 2014
recrystallized
SEI 20kV WD18mm SS46 x4,500 5μm
W ref. H: 1 shot 15 May 2014
deformed
SEI 20kV WD13mm SS46 x22,000 1μm
W deformed: 1 shot 15 May 2014
recrystallized
SEI 20kV WD18mm SS46 x4,300 5μm
W ref. H: 1 shot 15 May 2014

Experimental data

To be associated with dislocations ?

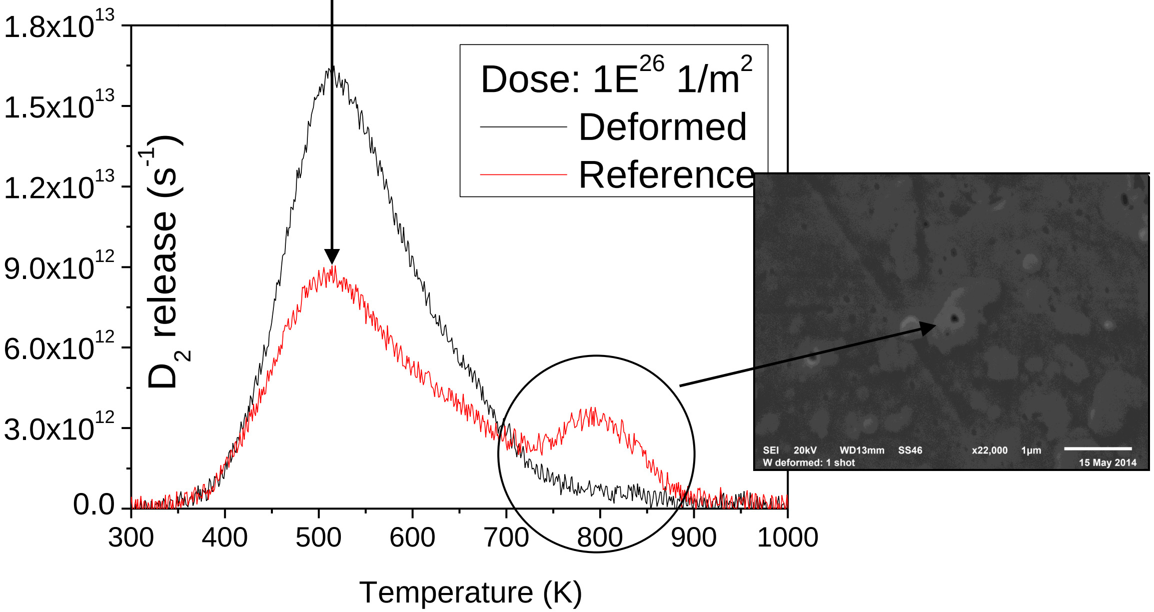

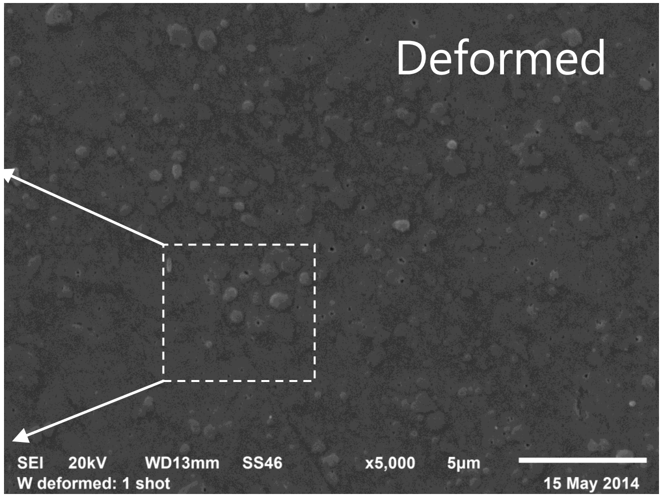

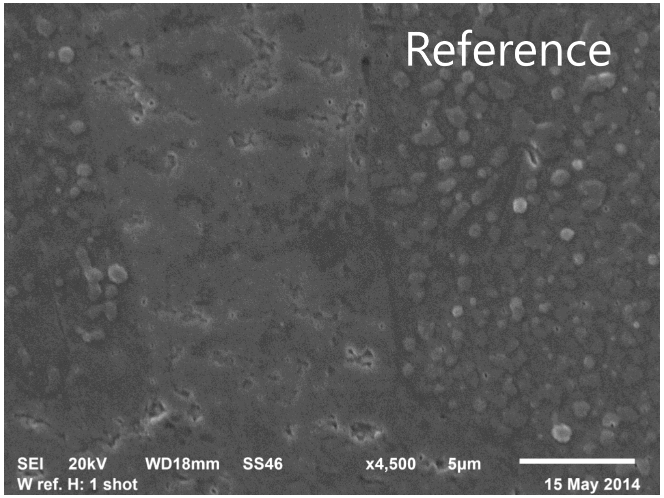

Absence of the high temperature peak !
... suppression or burst of blisters ?
Possible reasons:
- Shallower nucleation depth (burst)
- Internal stress (suppression of bubble growth by loop punching)

Experimental data

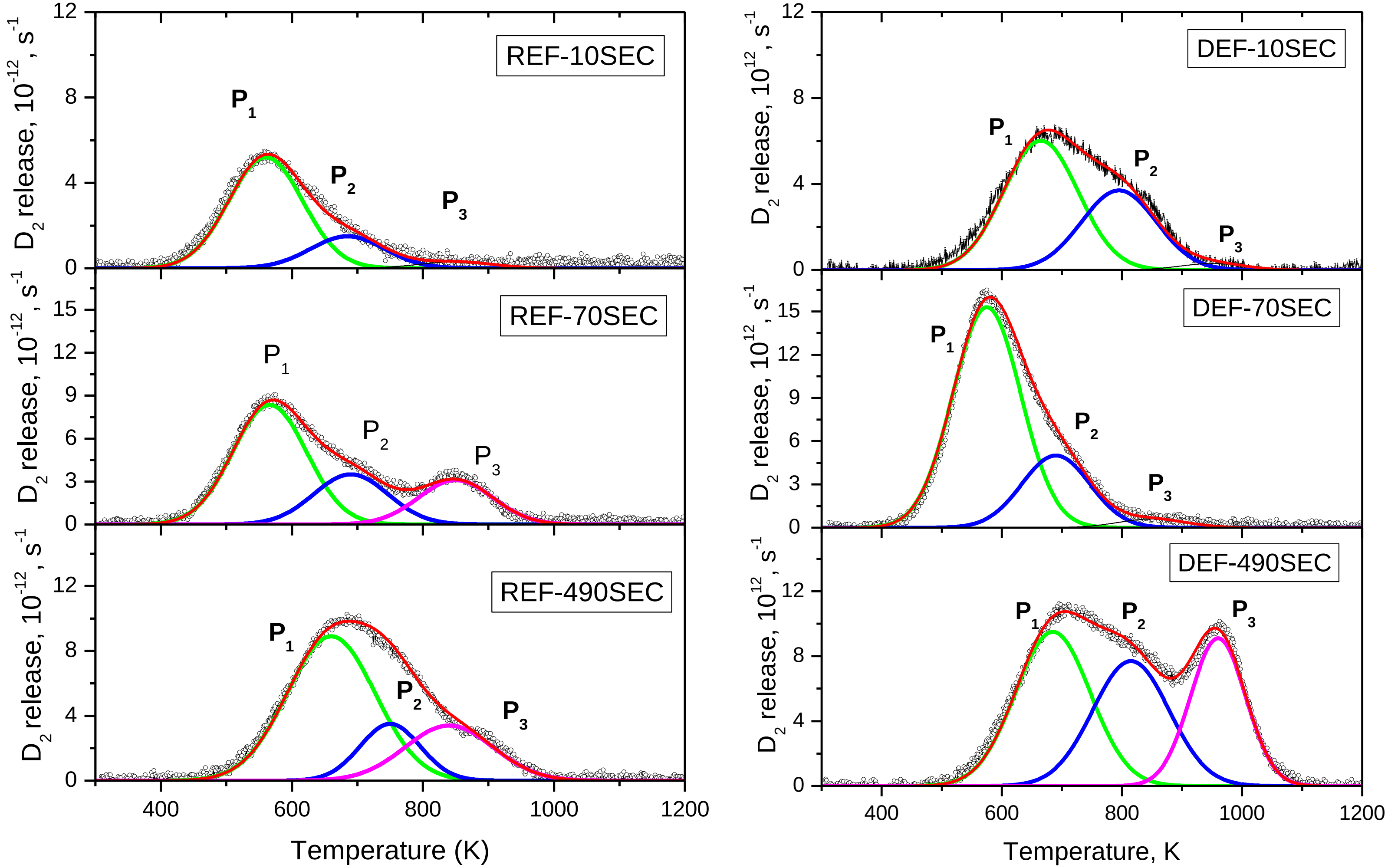

Experimental data

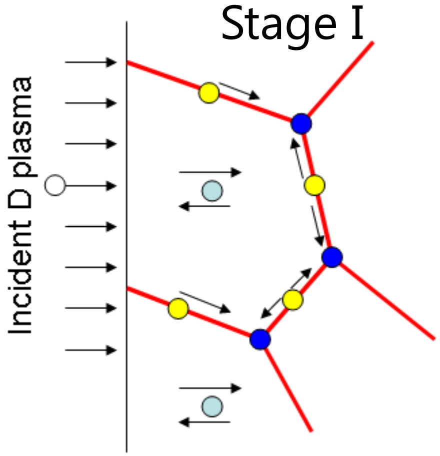

reference material

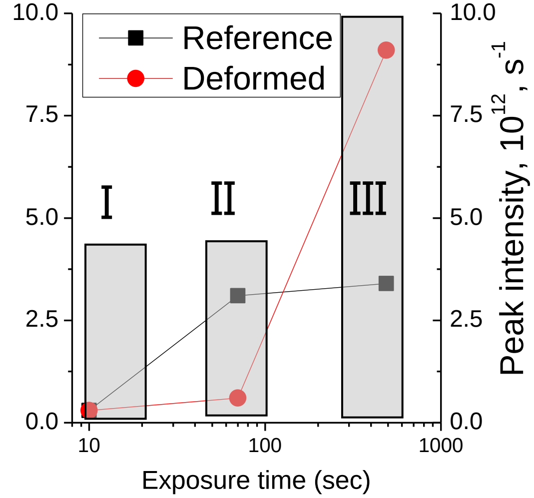

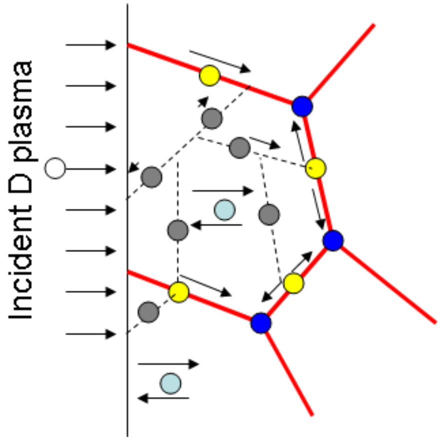

plastically deformed material

Legend:

- Dislocation
- GB interface
- D in plasma
- D in W bulk
- D in GB interface
- D in GB junction
- D at dislocation
- D in super-critical clusters
- D in sub-critical clusters

Plastic deformation promotes nucleation of H bubbles

Experimental data

- Our understanding of sub-surface trappin
  - Establishment of steady-state D profile
  - Compensation of compressive stresses by plastic deformation
  - Dislocation network acts as trapping & nucleation source
  - Nano-metric bubbles get to steady-state
- Pathway to validate/rationalize the hypothesis
  - Characterize trapping & nucleation on dislocations: atomistic sim.
  - Pass atomistic data to Mean Field (kinetic rate theory) for non-equilibrium nucleation
  - Combine with classical MF (diffusion limited)

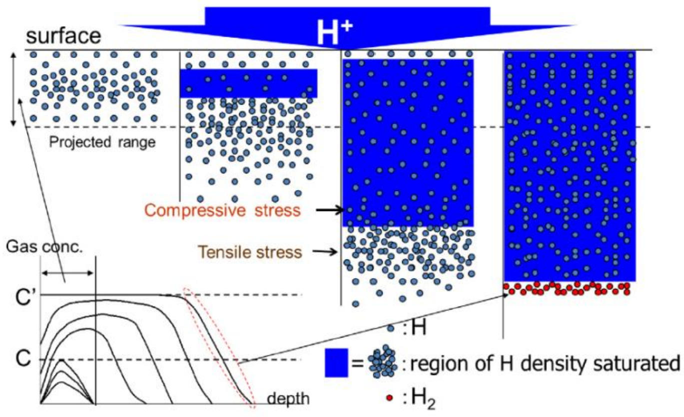

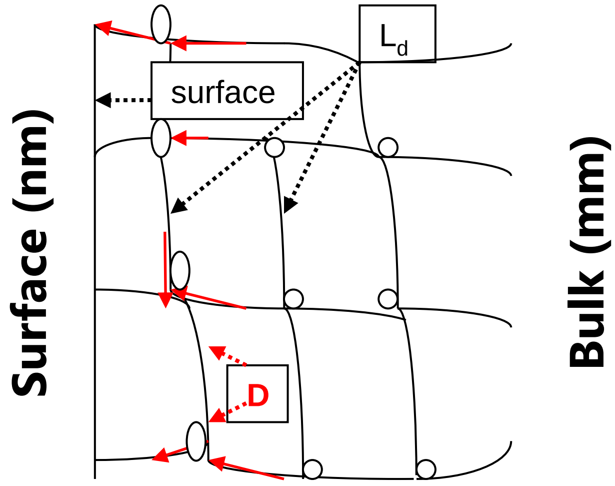

Hypothesis about trapping on dislocations

- Experimental and theoretical 'facts':
  - H-H do not form clusters: no self-trapping like for He
    - Binding (H-H)=0.02; (H_2-H)=0.01, (H_3-H)=0.02; (H_4-H)=0.03 eV **[1]**
  - Migration energy = 0.4 eV
    - H atom covers 30 μm within 1 ms: all permeated H immediately get trapped
  - Typical μ-structure of commercial W grades:
    - Dislocations, sub-grains, random grains
    - Porosity, Impurity
- Possible mechanisms of bubble nucleation <u>without vacancies</u>:

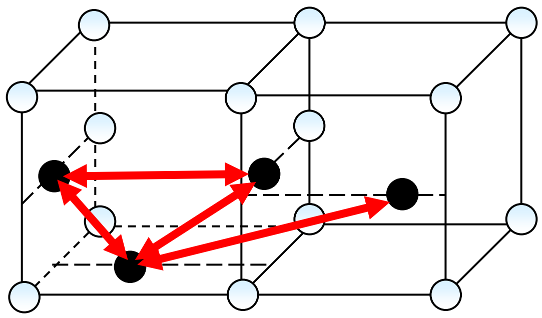

[1] K. Heinola, T. Ahlgren et.al., Physical Review B 82 (2010) 094102.

Interaction of Hydrogen with screw dislocation

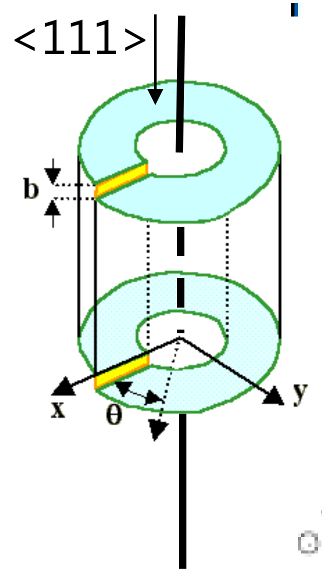

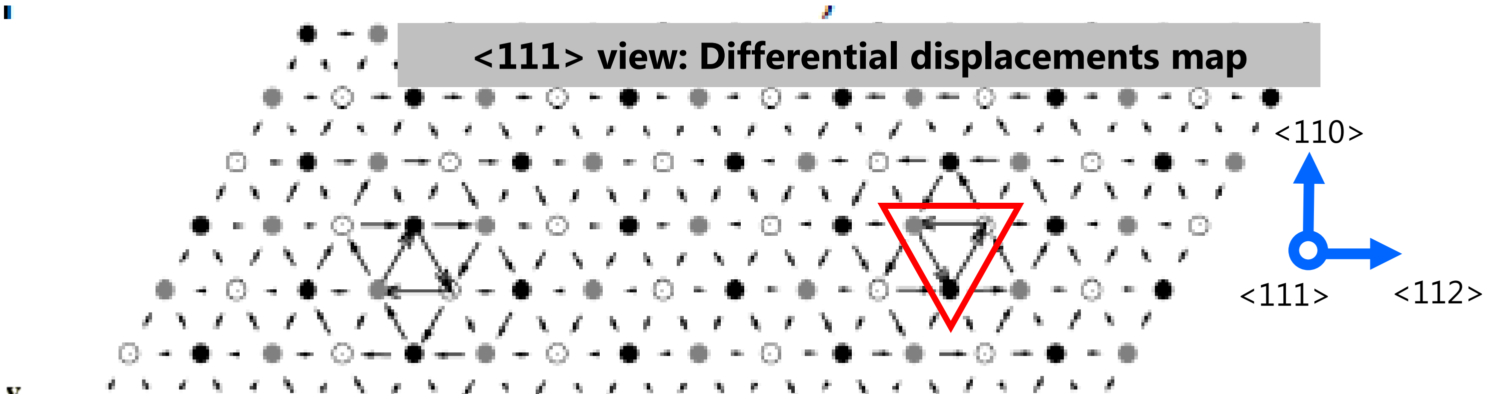

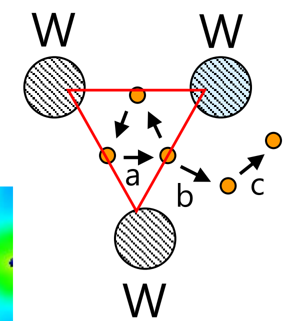

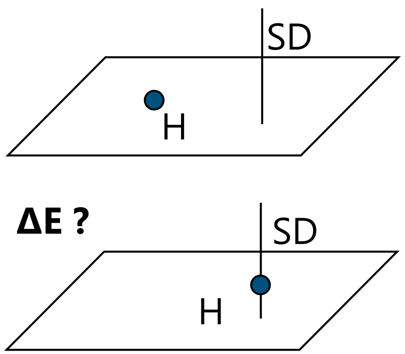

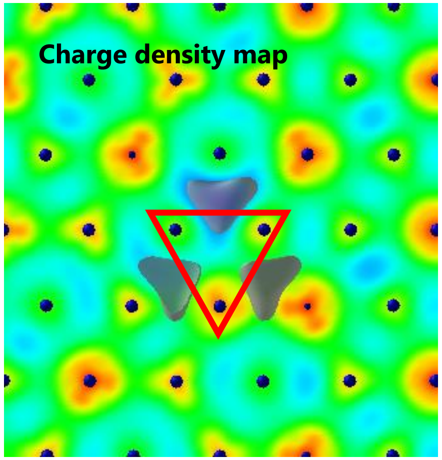

add H

ΔE = -0.6 eV

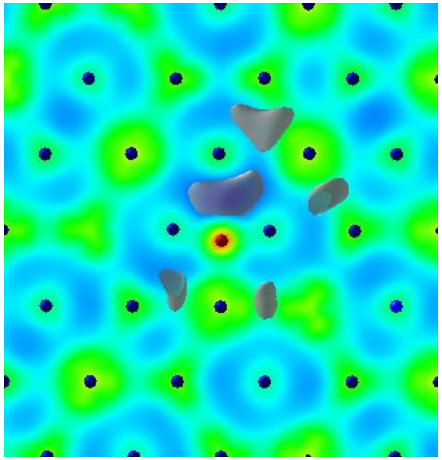

Migrations:

a – in core

b – in-out

c – out core

[1] D. Terentyev et.al. Nuclear Fusion Lett. 54 (2014) 042002.

Clustering of Hydrogen on screw dislocation

Binding energy [eV]

Size of H_N cluster	SD length=**b**
H + SD	-0.53
H + (H-SD)	-0.59
H + (H_2-SD)	-0.62
H + (H_3-SD)	-0.39
H + (H_4-SD)	-0.36

Charge density maps [e⁻/Å³]

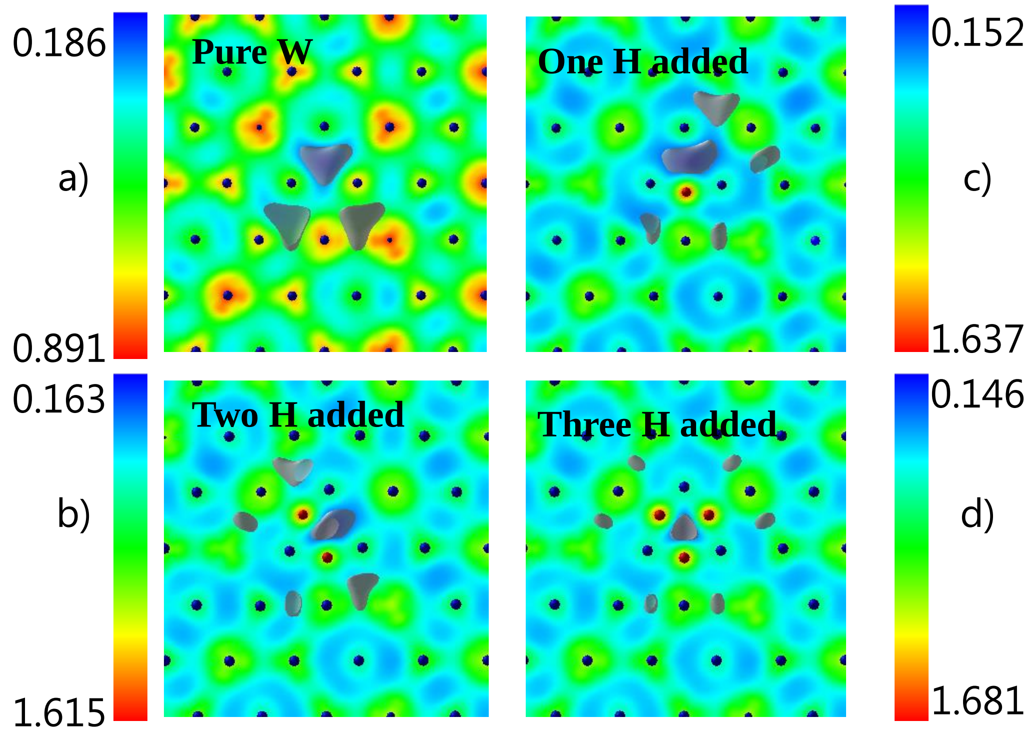

Screw dislocation can trap several hydrogen atoms simultaneously, but incremental binding energy decreases with number of trapped H atoms (from 0.6 – down to 0.25 eV).

[1] D. Terentyev et.al. Nuclear Fusion Lett. 54 (2014) 042002.

Nucleation of stable Hydrogen cluster on dislocation

Loop punching: growth of bubbles due to excess pressure via the emission of dislocation loops

A: Dislocation + cluster H_N

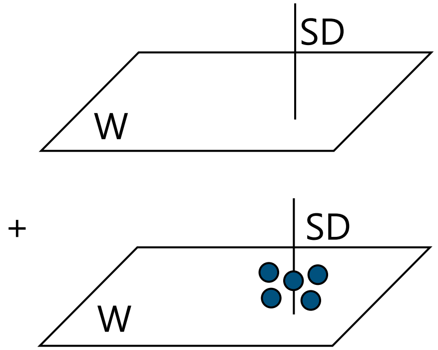

B: dislocation + (**Jog**—H_N) + **Jog**$^+$

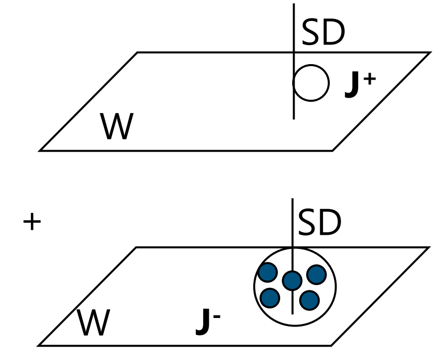

Classical loop punching mechanism

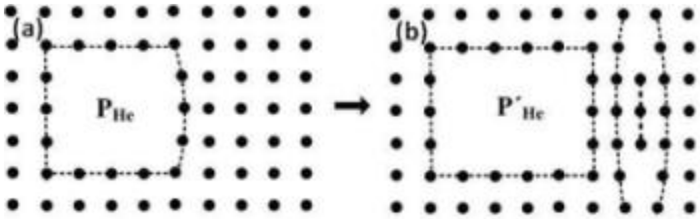

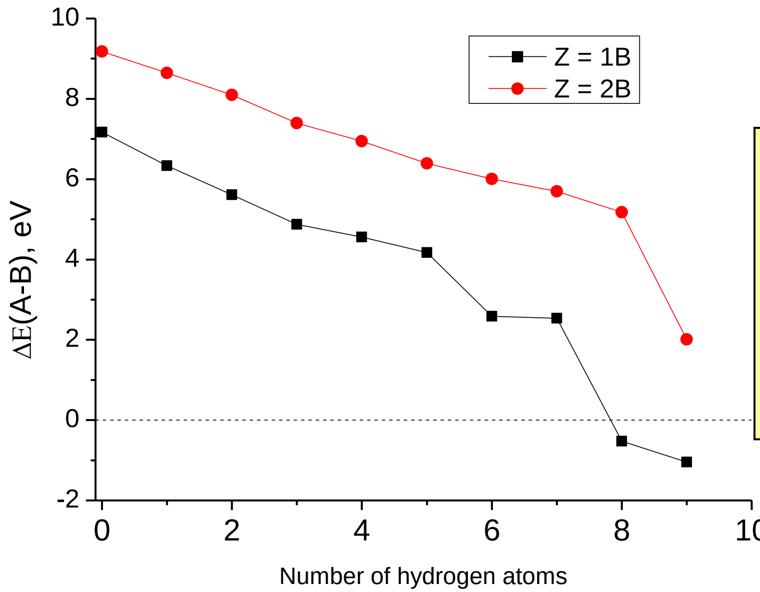

No attraction of H in bulk – no way to form critical concentration.

Clustering at dislocation core leads to jog emission at N_H=8

Jog punching: formation of vacancy jog to accommodate H_N cluster + emission of interstitial jog

Description of the model

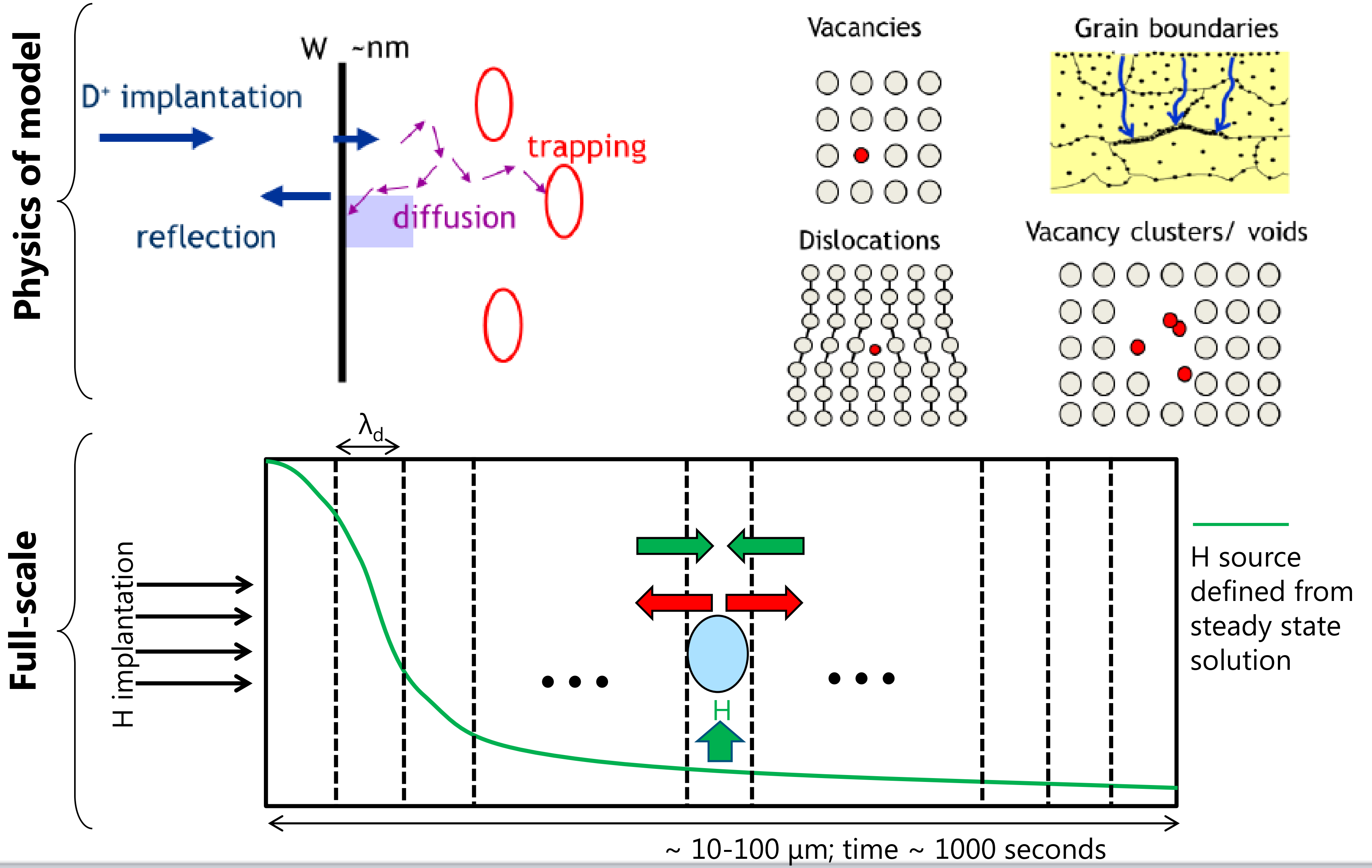

Computational model results & prototype tool

Estimation of experimental conditions for H bubble formation and surface blistering

- Steady state solution for diffusion in a field of traps
- $C(x) = C_0 \exp(-x k_D)$
- $k_D = \sqrt{\rho}$ for dislocations
- $k_{GB} \sim d$ for grain boundaries

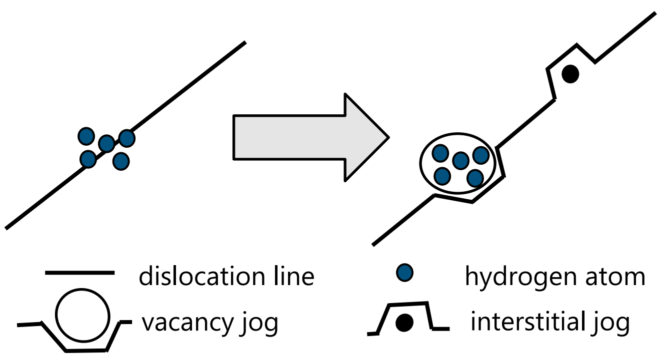

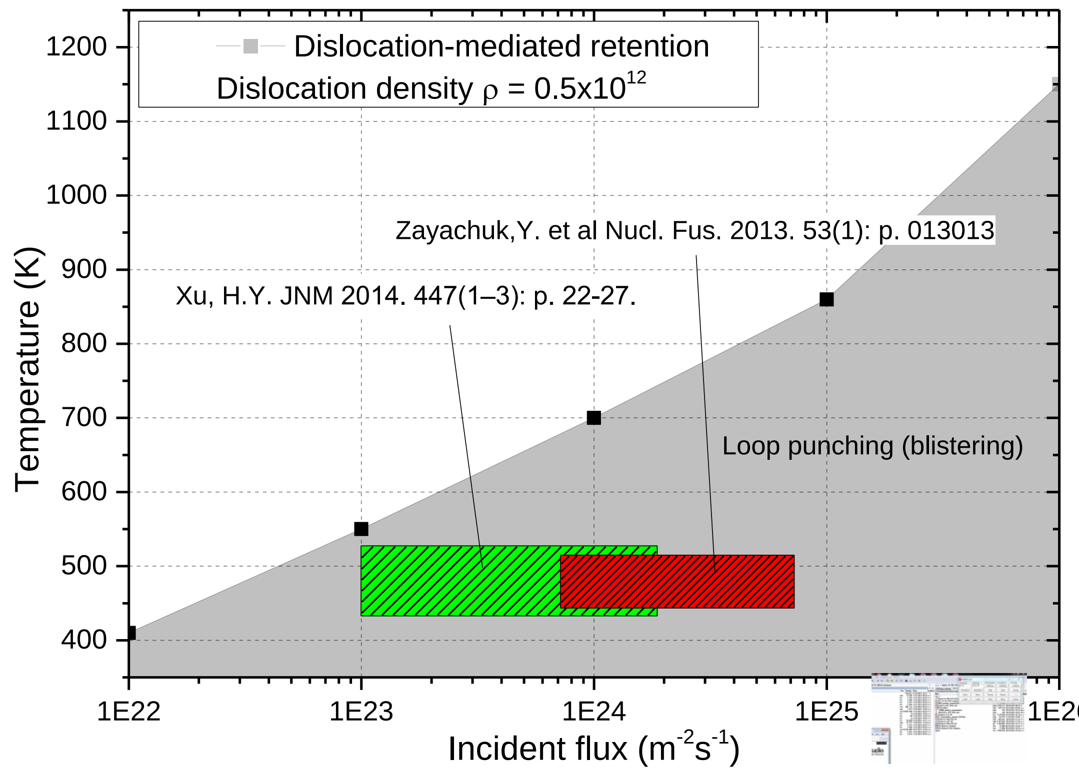

Model of H retention

- Two zoned retention
- Dynamic retention in sub surface region
- Trapping on natural defects in the bulk area

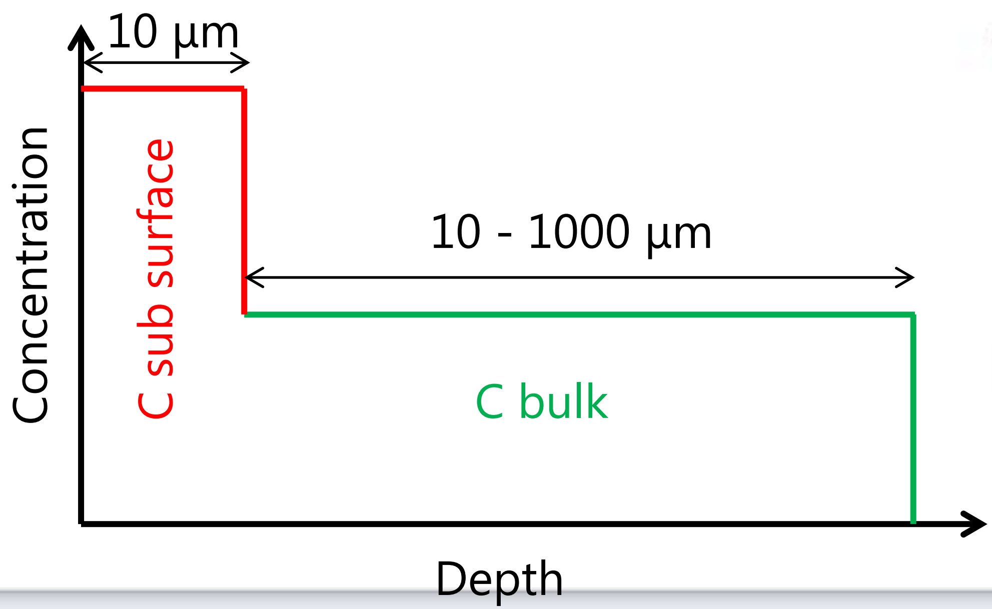

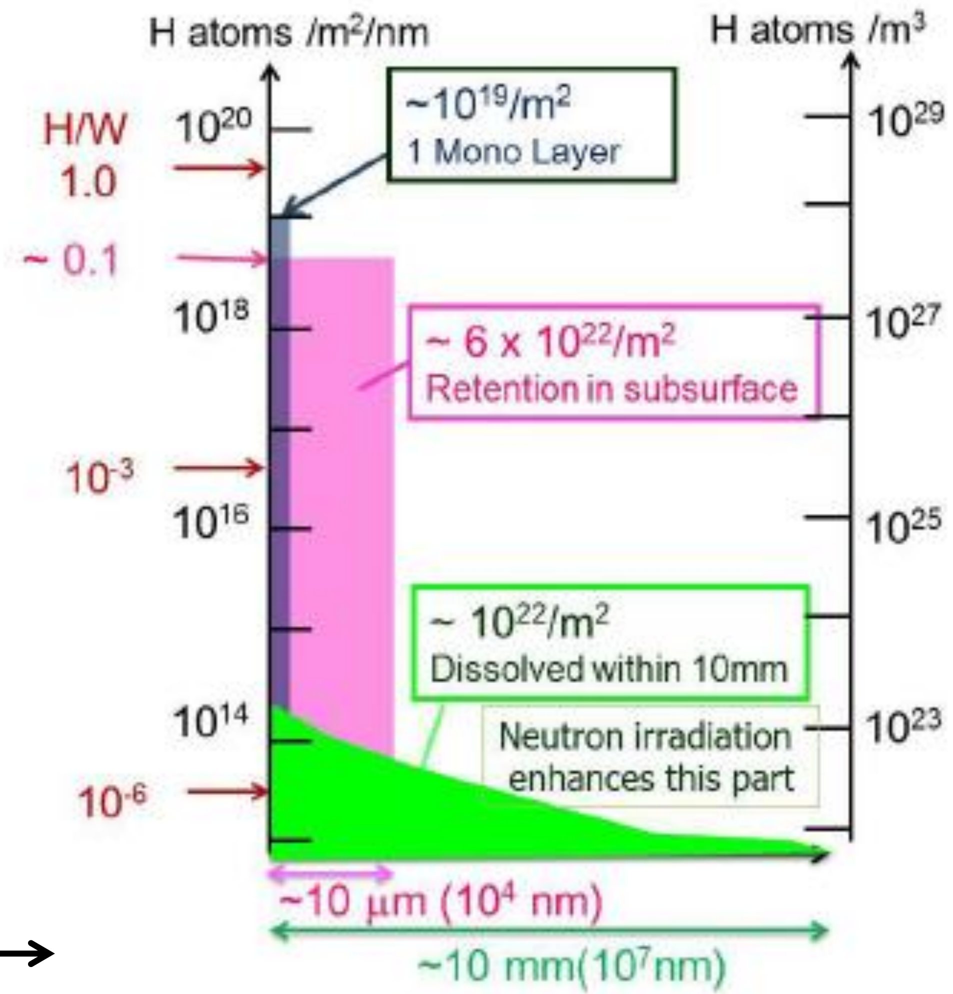

Release of trapped H

- Release from bulk and diffusion to the surface
- Concentration of H is defined by trapping and growth at low angle grain boundaries
- Binding energy of 2.0 eV

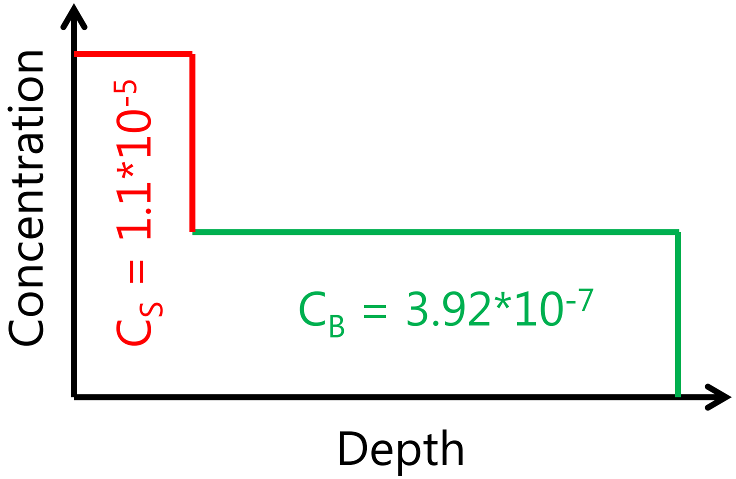

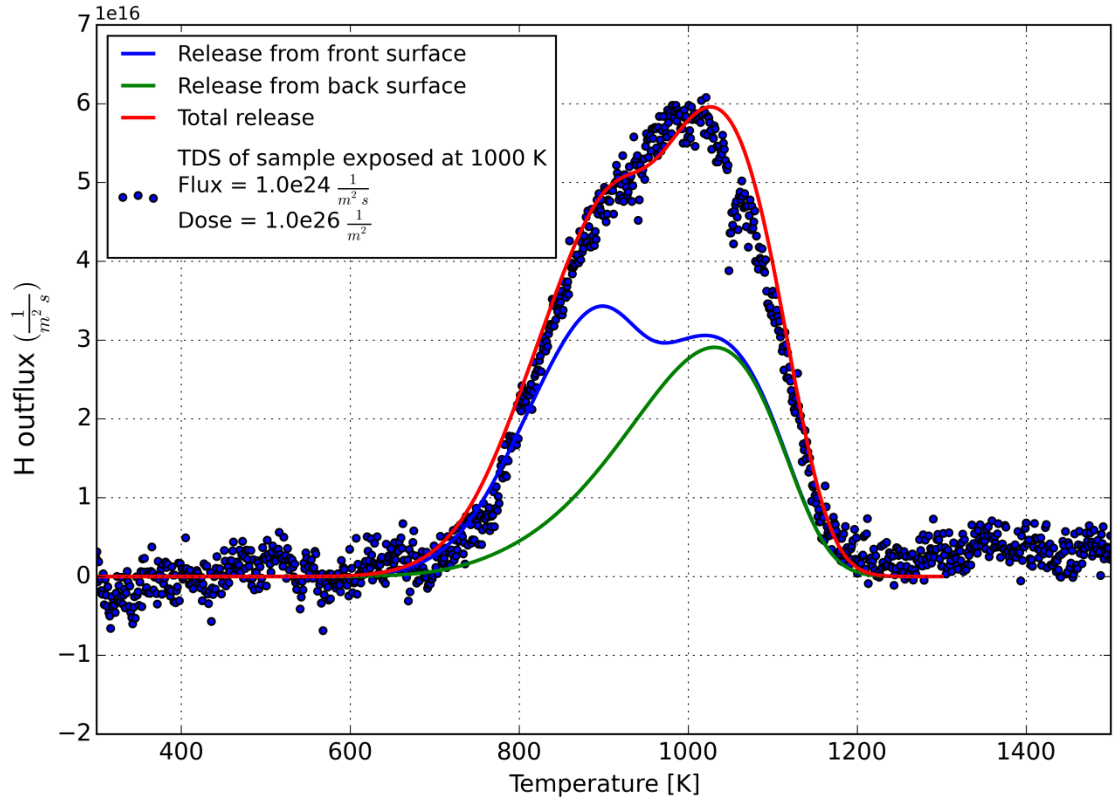

Part II

- Part II
  - Standard and improved high-Cr grades
  - Available improved 9-Cr batches
  - Preliminary tests including high flux plasma exposure

Radiation effects in structural materials

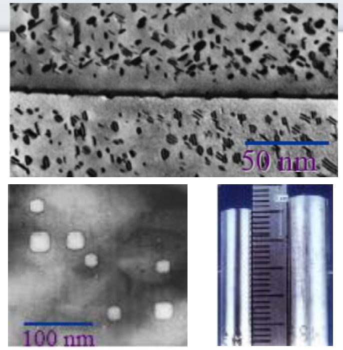

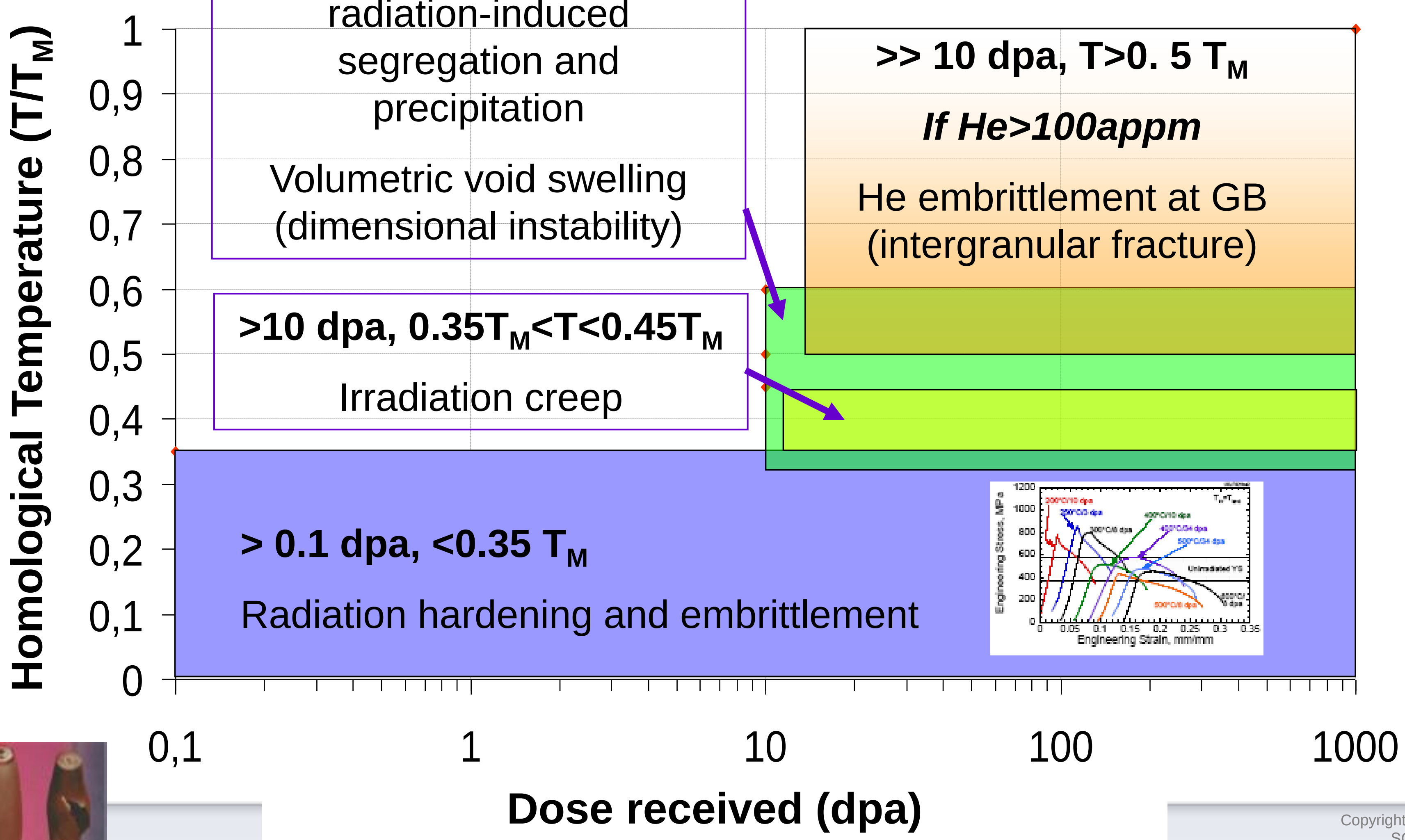

Standard and improved high-Cr grades for Fusion Appl.

- One principle problem of 9-Cr steels: low temperature embrittlement
- Second one: creep, limiting application up to 650C

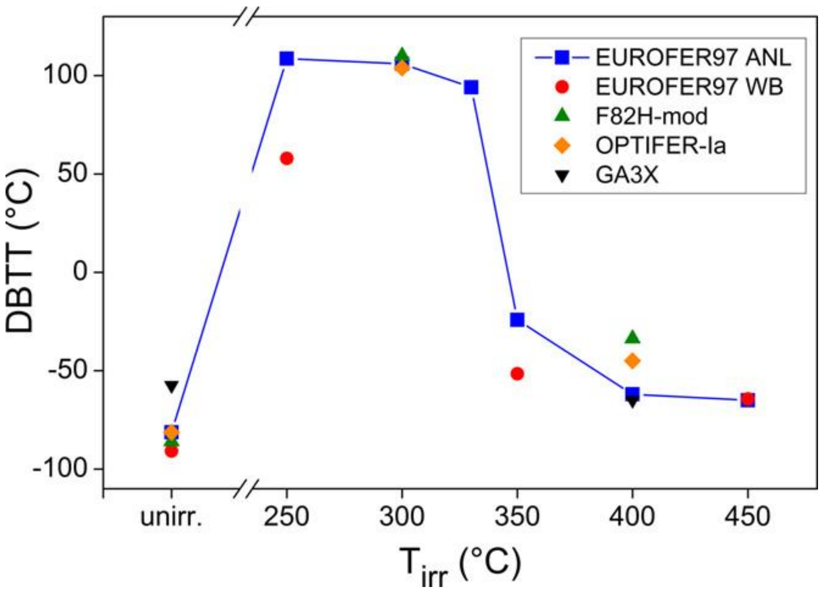

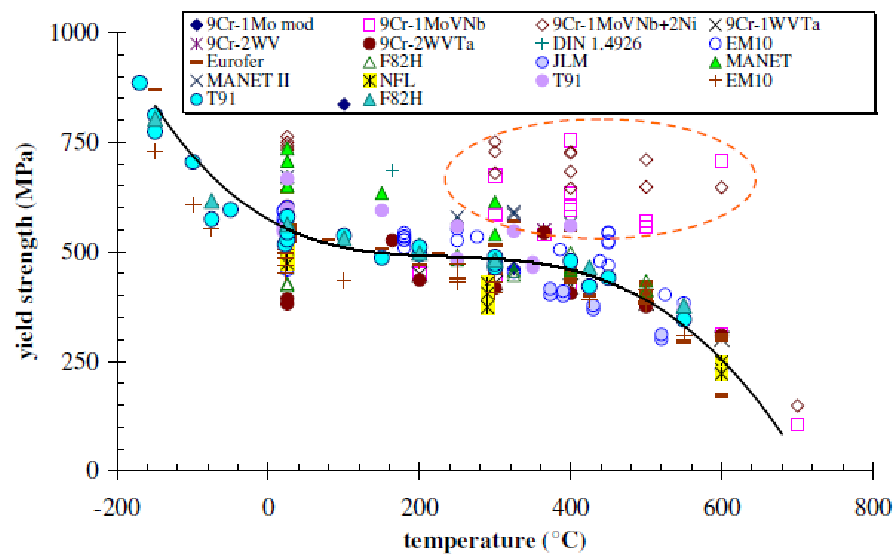

Steel	C	Si	Mn	Cr	Ni	Mo	W	V	Nb	B	N	Other
F82H	0.10	0.2	0.50	8.0			2.0	0.2		0.003		0.04 Ta
EUROFER	0.11	0.05	0.50	8.5			1.0	0.25		0.005		0.08 Ta

Standard and improved high-Cr grades for Fusion Appl.

- Plastic flow instability
  - Dynamic absorption of defects
  - Drastic softening of matrix

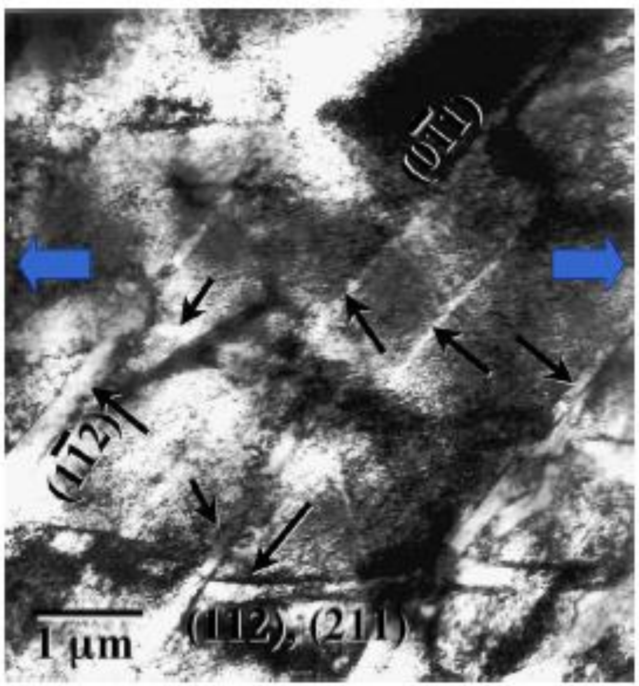

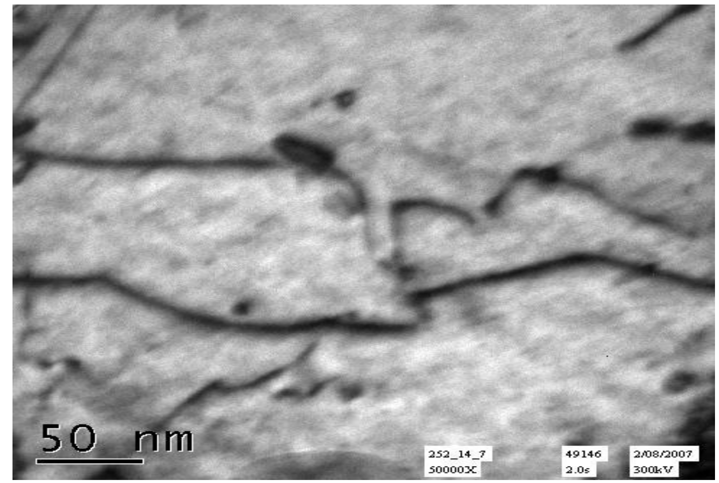

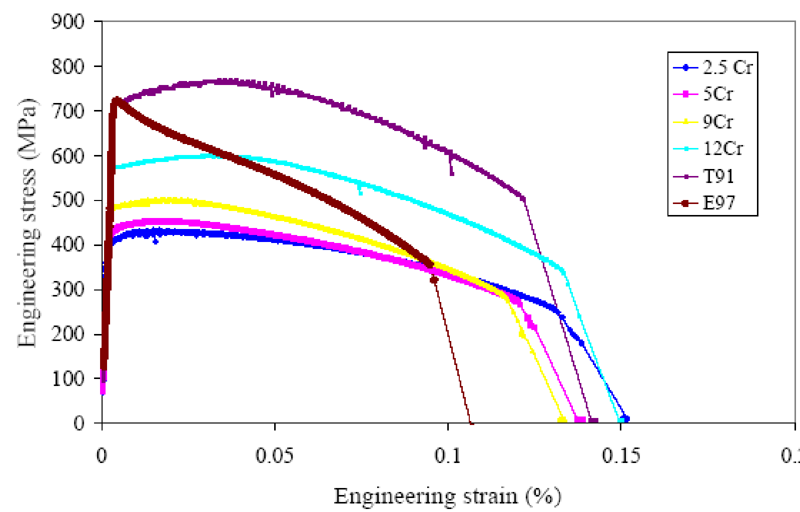

Journal of Nuclear Materials 351 (2006) 269–284

Development of new improved Eurofer grades

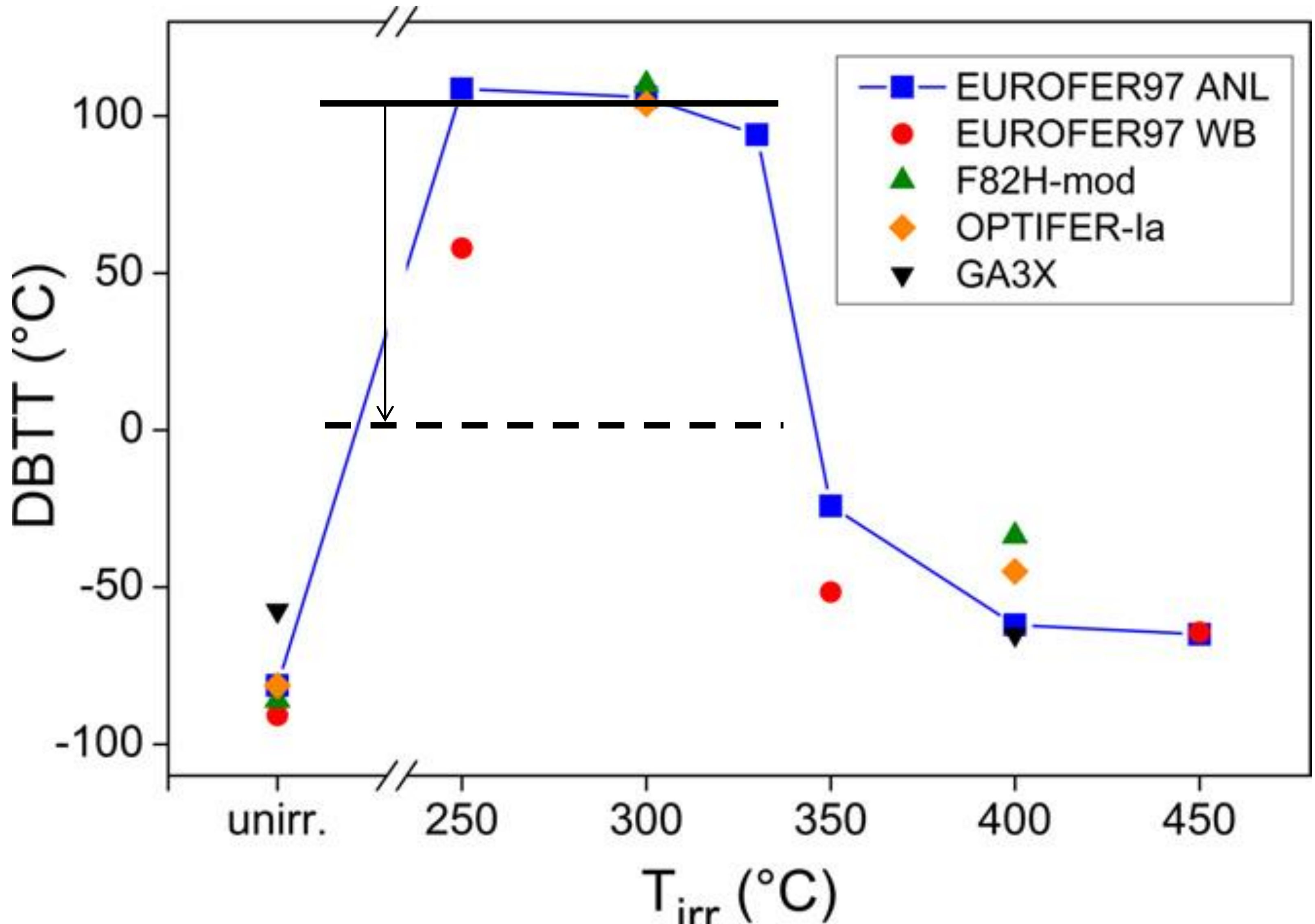

How to reduce DBTT and enhance creep resistance

- Modify precipitate distribution
  - Change ratio MC to MX
  - Modify H-treatment
  - Modify Composition
- V and Nb:
  - Stabilize grains
  - Reduce grain coarsening
  - Increase ductility
- 9Cr remains optimum
  - Less Cr – poor corrosion resist
  - More Cr – hardening (α’) and δ-ferrite

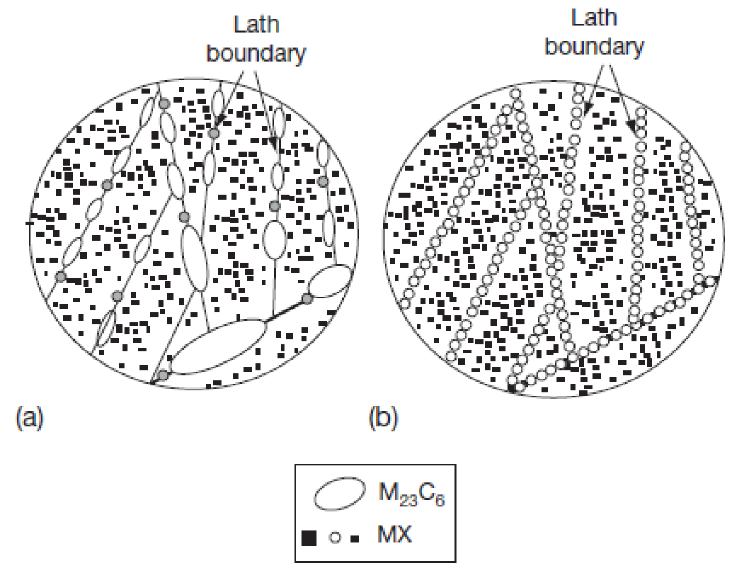

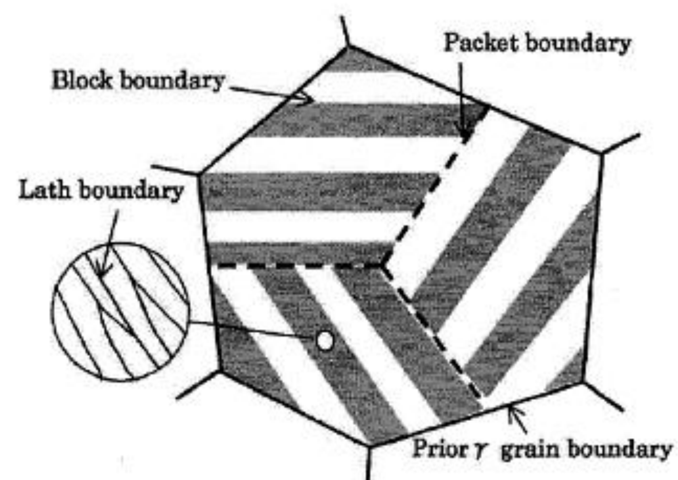

Advanced Thermo-Mechanical Treatment: TMT

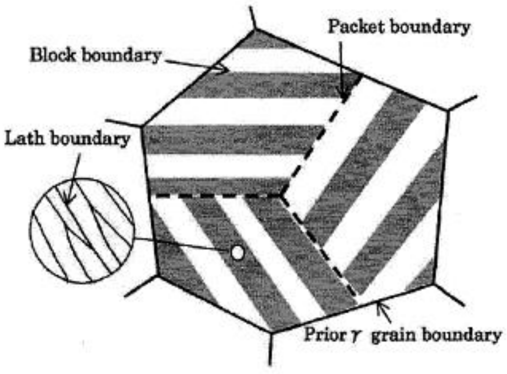

Experimental Procedure

Composition of the 9wt% Cr RAFM steel batches 2014

Wt%	C	Cr	Mn	N2	Ta	V	W
0.09Ta	0.11	9.13	0.40	0.011	0.09	0.23	1.04
0.11Ta	0.11	9.24	0.39	0.011	0.11	0.23	1.07

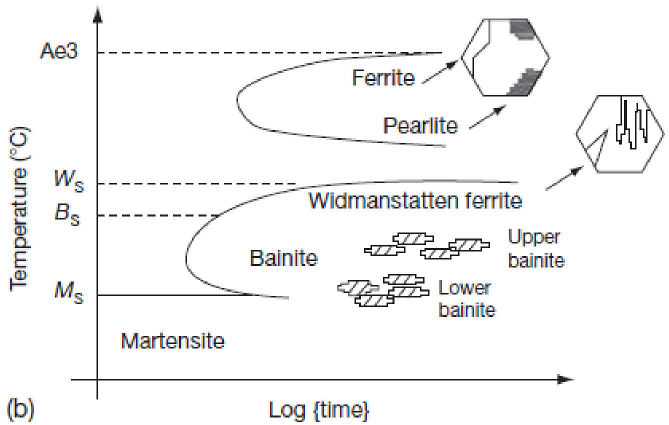

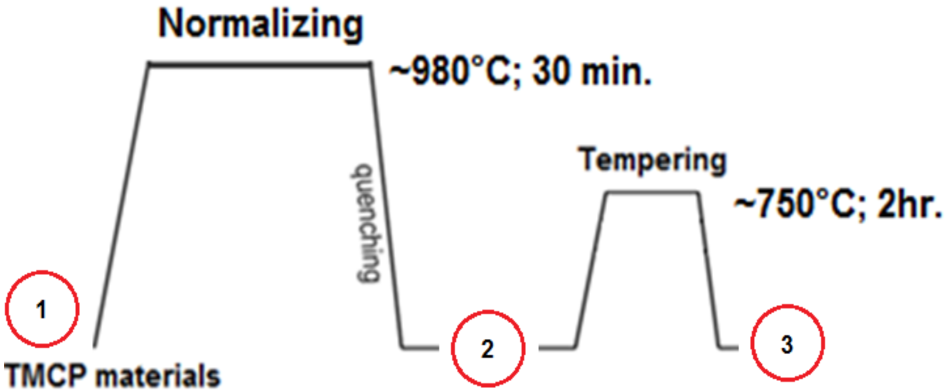

Advanced Thermo-Mechanical Treatment: TMT

0.09Ta

1

Pass 1		Pass 2		Pass 3		Pass 4		Pass 5		Pass 6	
T	%	T	%	T	%	T	%	T	%	T	%
1200	19.547	1150	25	1100	30	960	30	900	30	850	30

2

0.11Ta

Pass 1		Pass 2		Pass 3		Pass 4		Pass 5		Pass 6	
T	%	T	%	T	%	T	%	T	%	T	%
1220	21.978	1200	25	1180	30	1160	30	1140	30	1120	30

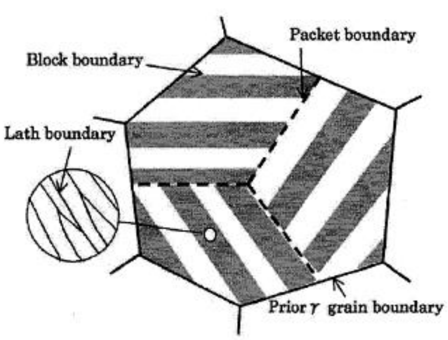

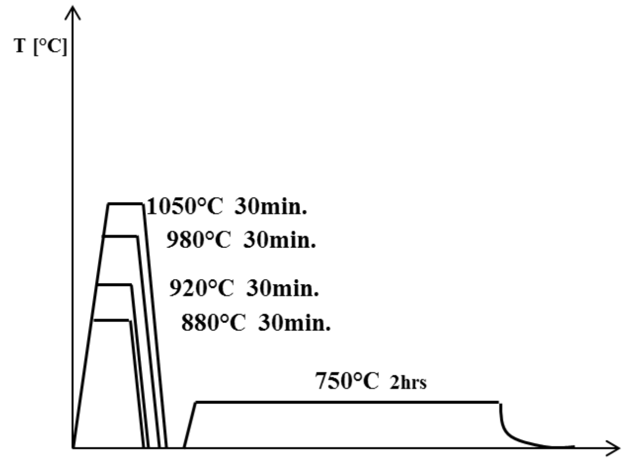

Effect of Heat Treatment

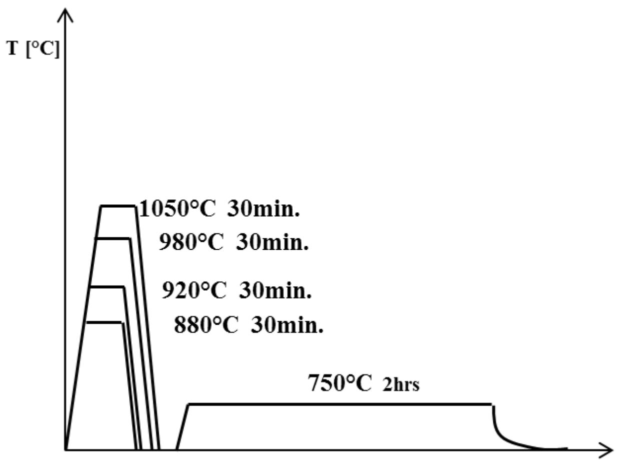

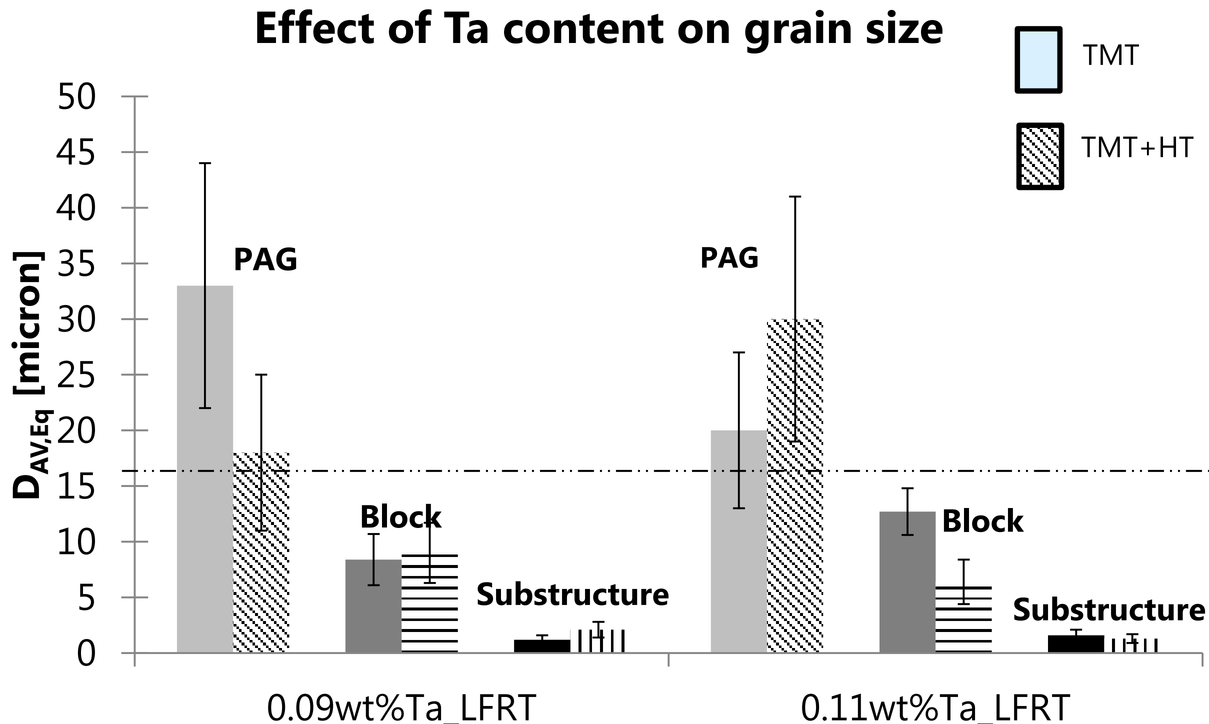

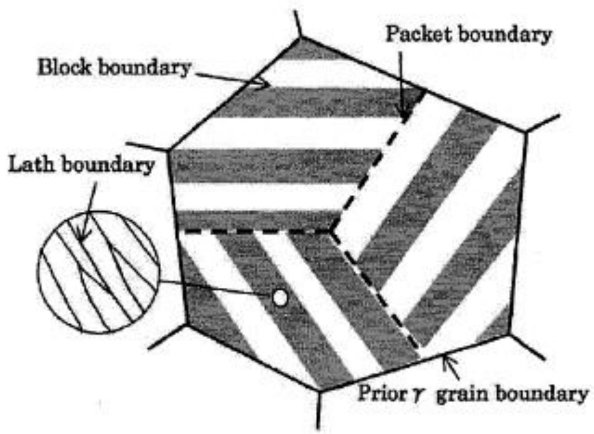

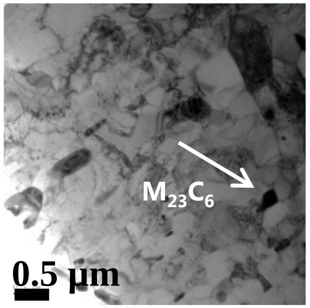

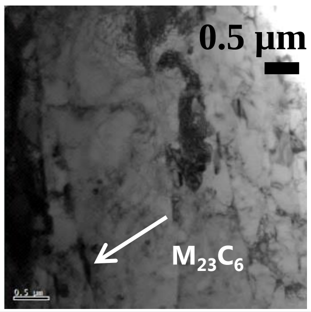

Precipitation of Vanadium and Tantalum

Fraction of elements that precipitate at different stages of Q&T treatment

Wt%	Cr	Ta	V
0.09Ta	9.3	0.086	0.22

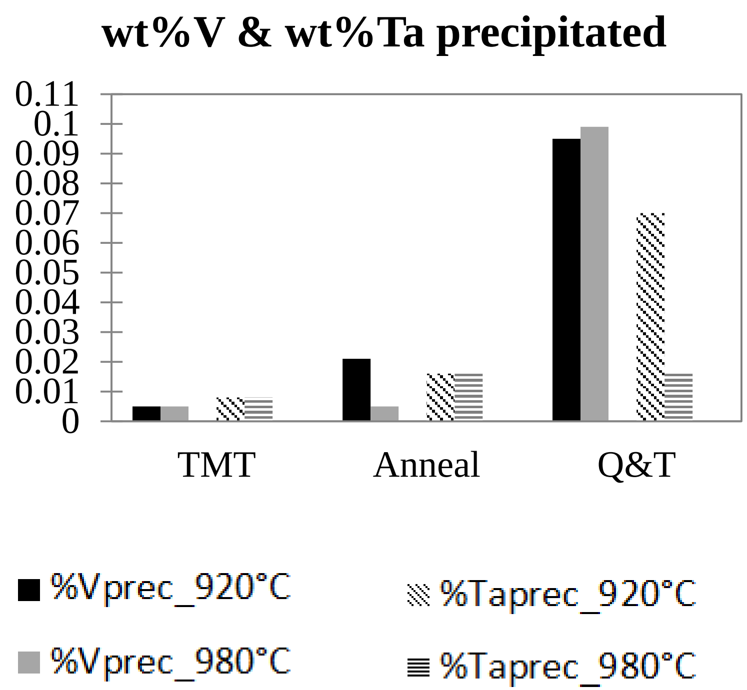

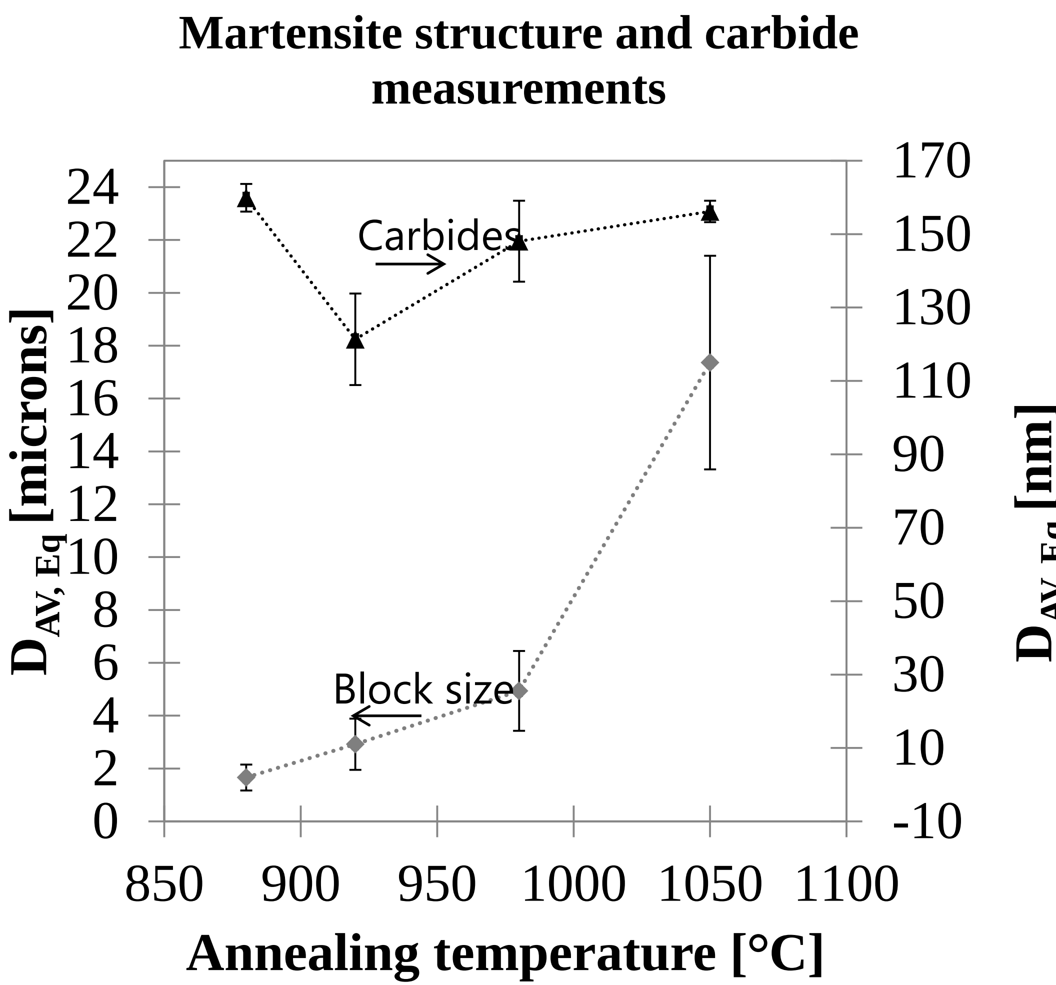

Mechanical properties of improved grades

Ultimate tensile strength

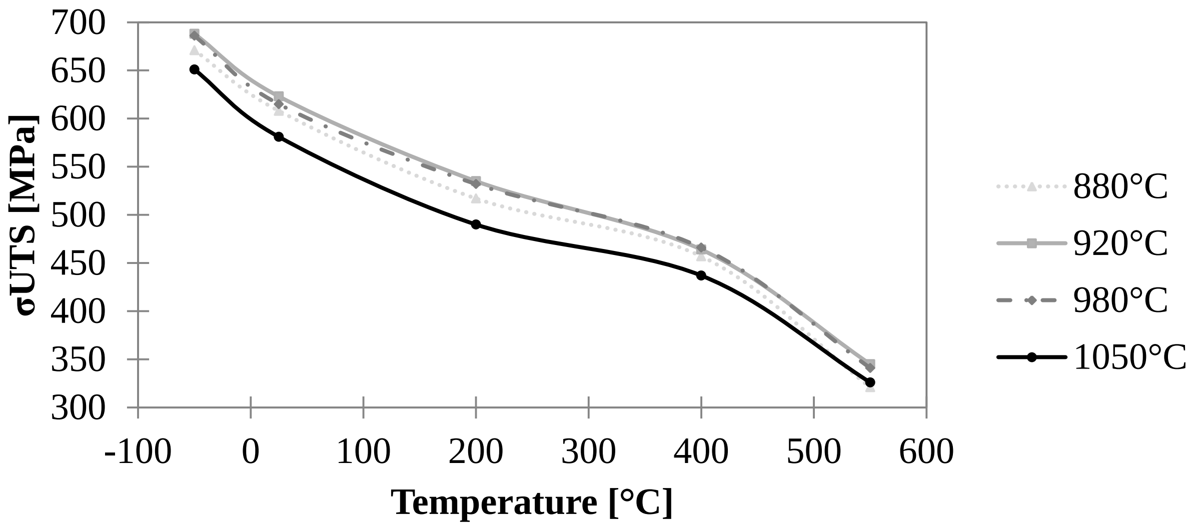

Q&T: 880°C tested at -140°C

Intermediate level

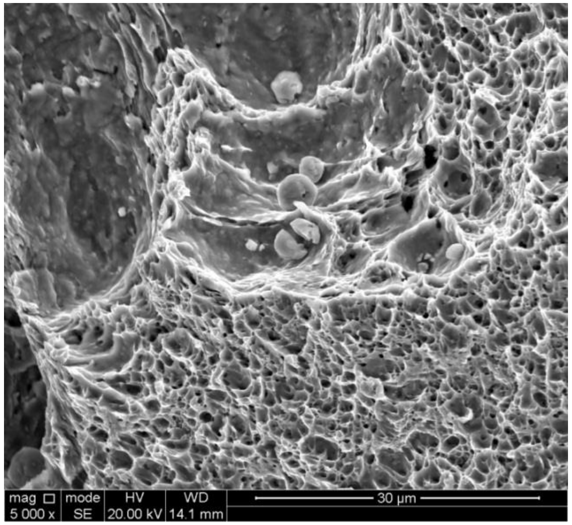

I196C - 880°C - KLST specimens

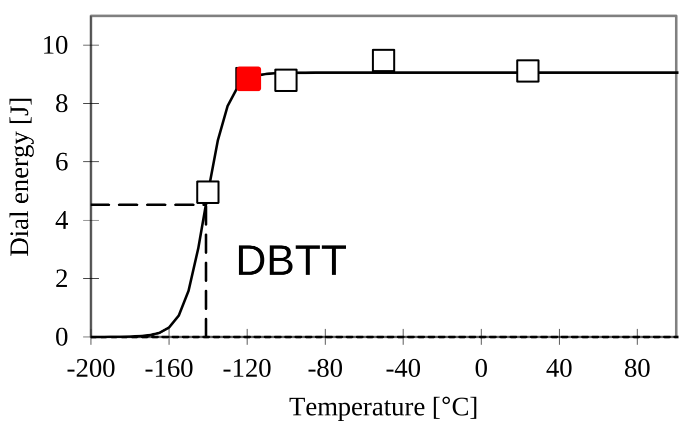

Q&T: 880°C tested at -120°C

Upper level

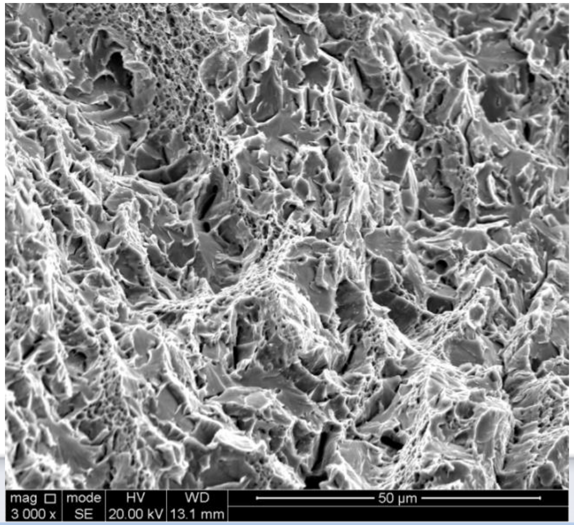

Preliminary results

- High Flux D plasma exposure at Pilot PSI (NL)
  - Surface temperature: 430-450K
  - Flux ~10^{24} D/m^2
  - Fluence ~5×10^{25} D/m^2
- Reference measurements
  - T91; E97

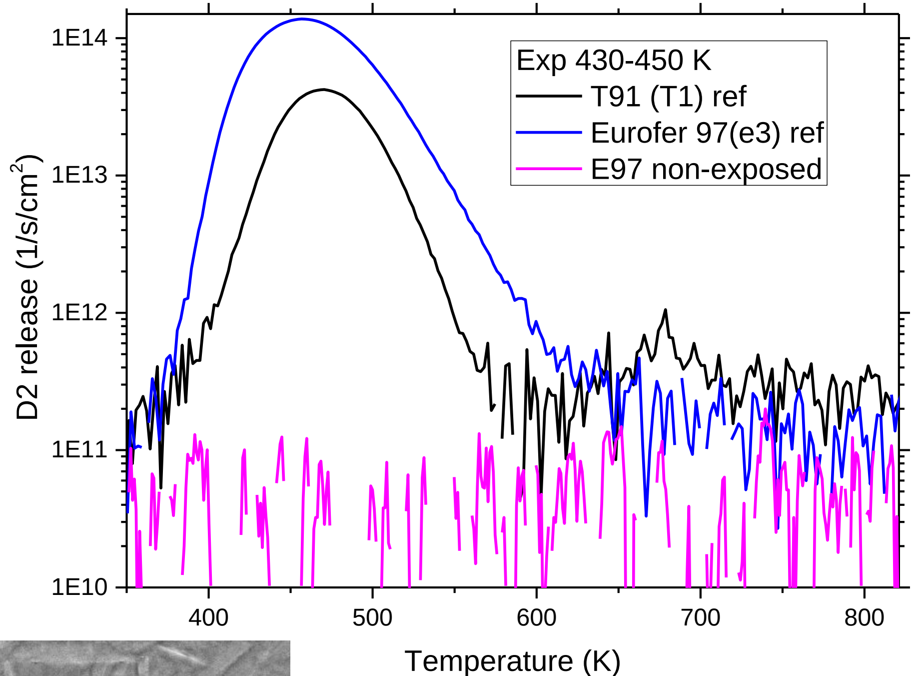

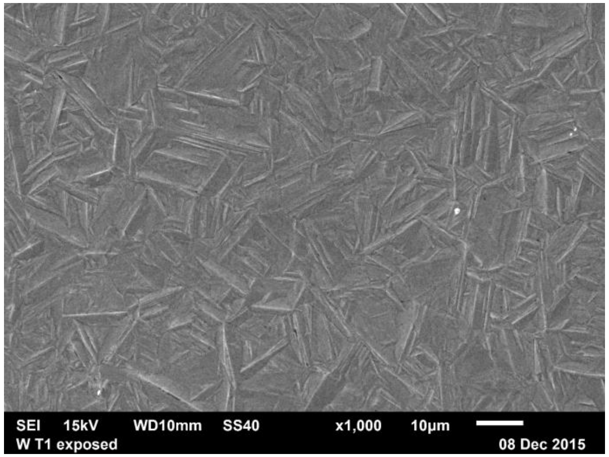

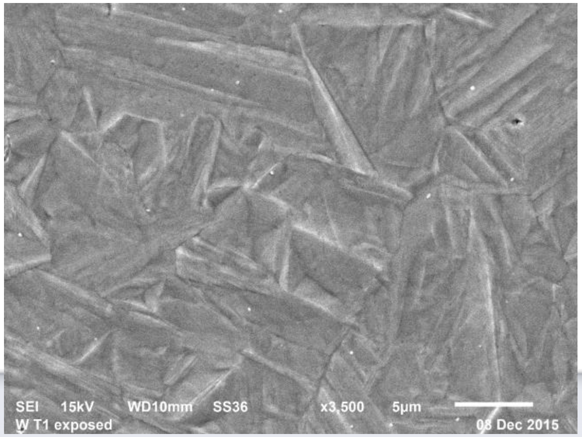

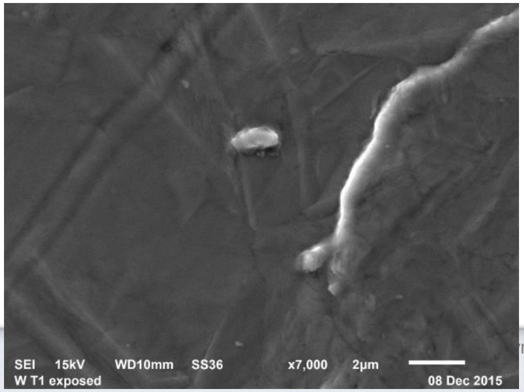

Preliminary results

- Exposure at 430-450K: Blisters and individual grains

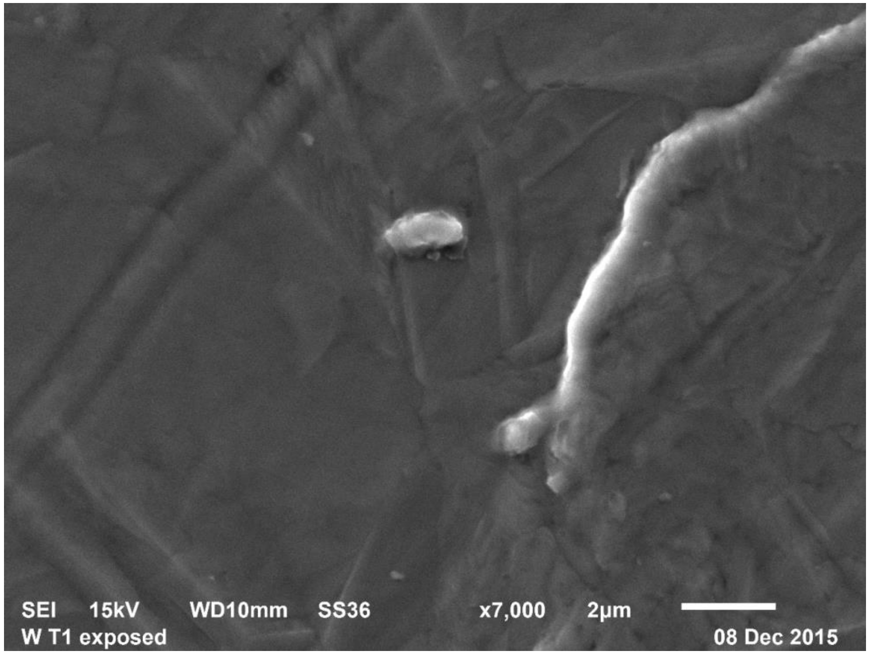

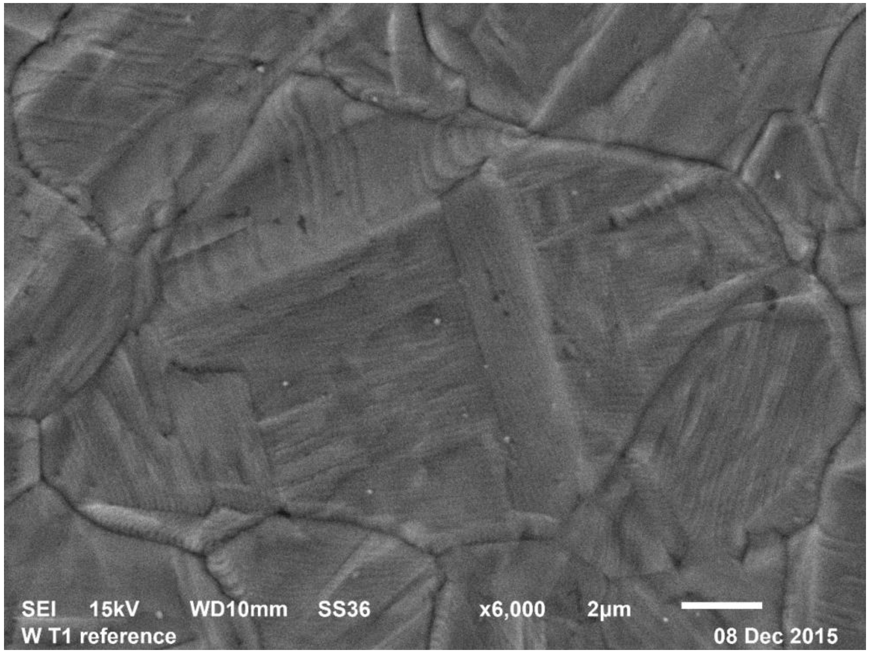

NRA/TEM analysis to be done to confirm sub-surface retention & µ-structure modification

Preliminary results

- Exposure at 430-450K: reference vs. advanced grade

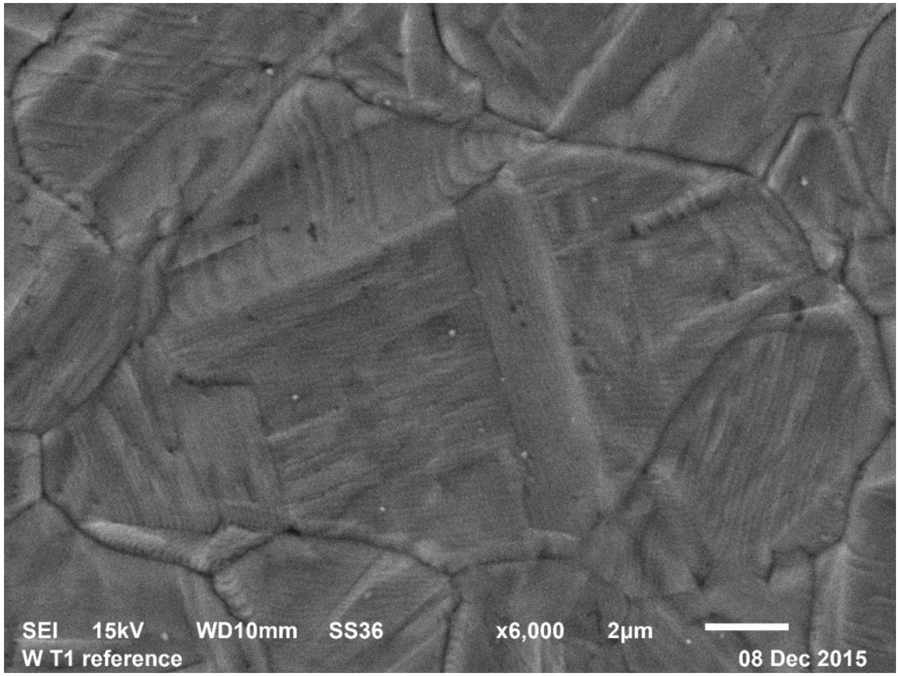

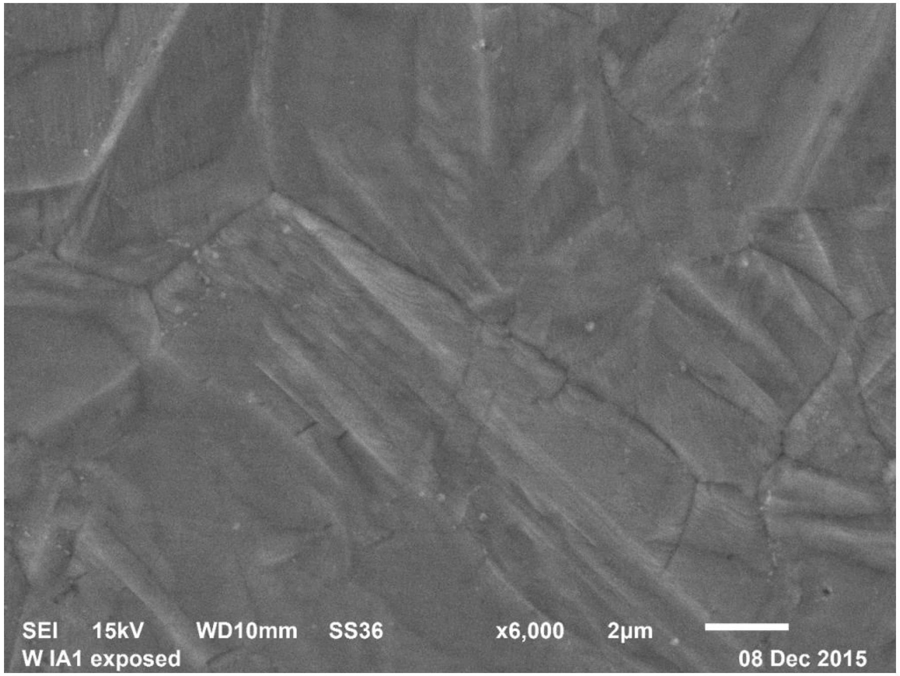

Chemical analysis to be done to confirm observations of Carbides at surface

Preliminary results

- High Flux D plasma exposure at Pilot PSI (NL)
  - Surface temperature: 950-970 K
  - Flux ~10^{24} D/m^2
  - Fluence ~5×10^{25} D/m^2
- Reference measurements
  - E97;